

Copyright
by
Hanjie Chen
2006

The Dissertation Committee for Hanjie Chen
certifies that this is the approved version of the following dissertation:

**INTEGRATED ENERGY RISK MANAGEMENT
MODELS FOR ELECTRIC UTILITY COMPANIES**

Committee:

Ross Baldick, Supervisor

Gustavo de Veciana

Mircea Driga

Yijun Du

Surya Santoso

**INTEGRATED ENERGY RISK MANAGEMENT
MODELS FOR ELECTRIC UTILITY COMPANIES**

by

Hanjie Chen, B.S., M.S.

DISSERTATION

Presented to the Faculty of the Graduate School of
The University of Texas at Austin
in Partial Fulfillment
of the Requirements
for the Degree of

DOCTOR OF PHILOSOPHY

THE UNIVERSITY OF TEXAS AT AUSTIN

December 2006

To my family.

Acknowledgments

I would like to gratefully and sincerely thank my supervisor, Dr. Ross Baldick, for his extraordinary patience, valuable guidance and suggestions so I am able to complete this dissertation. Dr. Ross Baldick has been of tremendous help in every aspect of my research abilities from modeling skills down to academic writing. I would also like to thank Dr. Yijun Du from the Lower Colorado River Authority (LCRA). He shared years of research and experience in the energy industry since the beginning of my career in LCRA as an intern in his group and I have learned a lot from him.

I am lucky to be a member of Energy Systems of Electrical and Computer Engineering Department at The University of Texas at Austin, where I had the chance to work with many wonderful people including Dr. Martin L. Baughman and Dr. John N. Jiang, who have been very helpful from the very beginning of my graduate study. I also thank the other members in my dissertation committee for their help.

Specially thanks to my girl friend, Jun Xia, and my family including my father, Xingchi Chen, my step-mother, Chuyun Luo, and my brother, Hanrui Chen, for their unending understanding and support throughout my graduate study. I really wish my mother, Bixuan Huang, were able to live till today to see my work, but I am sure she is happy to know it from the Heaven.

INTEGRATED ENERGY RISK MANAGEMENT MODELS FOR ELECTRIC UTILITY COMPANIES

Publication No. _____

Hanjie Chen, Ph.D.

The University of Texas at Austin, 2006

Supervisor: Ross Baldick

This dissertation presents models for integrated energy risk management for electric utility companies (EUCs). First, two fundamental market factors in deregulated electricity markets (electricity demand and price) are proposed and detailed studies of the correlation between electricity load and natural gas price reveals some interesting results. Second, an optimal natural gas supply selection framework based on modern utility theory is proposed. The framework is the first integrated risk management model to address the optimal fuel supply problem, which has been much more difficult and critical to EUCs in deregulated electricity markets. The framework can be extended for use in various time frame and as a benchmarking tool for trader's strategy. Thirdly, a framework to determine the feasible structures and find out the optimal insurance on generation forced outages (IGFO) contracts for EUCs is developed and its benefits to EUCs are discussed.

Table of Contents

Acknowledgments	v
Abstract	vi
List of Tables	xi
List of Figures	xii
Chapter 1. Introduction	1
1.1 Background	1
1.2 Literature Review	2
1.3 Motivation	8
1.3.1 Market Fundamental Analysis	8
1.3.2 Integrated Supply Optimization	10
1.3.3 Risk Management Practice	11
1.4 Dissertation Organization	11
Chapter 2. Modeling the Fundamentals in Deregulated Electricity Market	13
2.1 STLF using Knowledge Based ARX Models	14
2.1.1 Knowledge-Based Weather Segmentations	16
2.1.2 Scheme for Model Development and Application	17
2.1.3 Application	18
2.2 Electricity Price Dynamics	23
2.2.1 Suggestions of Economic Research	23
2.2.2 Empirical Investigation Results	25
2.2.3 Observations Summary	31
2.3 Correlation between HSC Natural Gas Spot Price and ERCOT Electricity Demand	32

2.3.1	Data Description	33
2.3.2	Overall Analysis	33
2.3.3	Natural Gas Supply and Demand Factor	36
	2.3.3.1 Injection Season	37
	2.3.3.2 Withdrawal Season	39
2.3.4	Conclusions	46
	2.3.4.1 General Conclusion	46
	2.3.4.2 Specific Conclusion	47
Chapter 3. Short-Term Natural Gas Supply Optimization		48
3.1	Introduction	49
3.2	Risk Characterization	51
	3.2.1 Volatility in natural gas spot markets	51
	3.2.2 Volatility in natural gas demands	52
3.3	Risk-Cost Framework	54
3.4	Modeling Approach	56
	3.4.1 Interaction with Markets	56
	3.4.2 Natural Gas Products in Current Markets	57
	3.4.3 Storage Gas (SG)	59
	3.4.4 Daily cost of natural gas	60
	3.4.5 Risk preferences of EUCs	61
	3.4.6 Objective function	62
	3.4.7 Integrated simulation-optimization algorithm	63
3.5	Applications	63
	3.5.1 Model setup	64
	3.5.2 Modeling risk preferences	68
	3.5.3 Results and discussions	68
3.6	Conclusions	73

Chapter 4. Determining Optimal Structure for Insurance on Generation Forced Outage	74
4.1 Introduction	75
4.2 Evaluation of IGFO Contracts	77
4.3 Optimal Choice of Feasible IGFO Structure	79
4.3.1 Definition	80
4.3.2 Decomposition of Payout Distribution	82
4.3.3 Feasible Structure	82
4.3.4 Optimal IGFO Structure	84
4.4 Numerical Application	85
4.4.1 Case Setup and simulation results	85
4.4.2 Feasible IGFO Structures	86
4.4.3 Caveats	90
4.5 Factors Affecting FSI	91
4.5.1 Risk Tolerance Contrast Ratio	91
4.5.2 Price Volatilities	93
4.5.3 Insurance Aggregation	94
4.6 Conclusions	96
Chapter 5. Conclusions and Future Research	98
5.1 Summary of Current Results	98
5.2 Integrated Risk Management Framework	100
5.2.1 Traditional Approach	100
5.2.2 Transition to Deregulation Markets	101
5.2.3 Utility Maximization Based Framework	103
5.3 Future Research	106
5.3.1 Integrated Risk Management Framework	106
5.3.2 Other Issues	108
Appendix	110
Appendix 1. Visual C++ Code for IGFO Simulator	111
Bibliography	136

List of Tables

2.1	Comparisons of Both Models for the First Test Week	20
2.2	Comparisons of Both Models for the Second Test Week	21
2.3	WMAPE and Standard Deviation for Both Weeks	22
2.4	DAMPE and WMAPE of All Models for the Second Test Week	22
3.1	Comparisons of results from three methods	72
4.1	Decomposition Results	86
4.2	Distribution Decomposition for Not Insured	87
4.3	Upper Bound Prices of IGFO Contracts for the EUC ($\times 1,000$)	88
4.4	Expected Payouts of Different IGFO Contracts ($\times 1,000$)	88
4.5	Probabilities of IGFO Payouts to Exceed the Upper Bound Price	88
4.6	Minimum Prices of IGFO Contracts for the Insurer ($\times 1,000$)	89
4.7	FSI and Utility for Different IGFO Contracts ($\times 1,000$)	89
4.8	FSI for Different IGFO contract ($\times 1,000$)	92

List of Figures

2.1	Scheme of Developing Forecasting System.	17
2.2	Scheme of Applying Forecasting System.	18
2.3	Forecast Comparisons for the First Test Week	20
2.4	Forecast Comparisons for the Second Test Week	21
2.5	Dynamic Evolution of the Electricity Spot Market Price	24
2.6	Existence of Price Jump Threshold	28
2.7	Time series of market demand, GFO capacity and price index	29
2.8	SLCR and SGFO in the Price Dynamics	30
2.9	ERCOT Daily Consumptions and Natural Gas Spot Prices . .	34
2.10	ERCOT daily electricity consumption vs. ln natural gas daily spot price from 1998 to 2005	34
2.11	ERCOT daily electricity consumption vs. ln natural gas daily spot price from 1998 to 2002	35
2.12	ERCOT daily electricity consumption vs. ln natural gas daily spot price from 2003 to 2005	35
2.13	ln Natural gas spot price vs. ERCOT energy demand at injec- tion season, 1998-2005	38
2.14	ln Natural gas spot price vs. ERCOT energy demand at injec- tion season, 1998-2002	38
2.15	ln Natural gas spot price vs. ERCOT energy demand at injec- tion season, 2003-2005	39
2.16	ln Natural gas spot price vs. ERCOT energy demand - with- drawal season	40
2.17	ln Natural gas spot price vs. ERCOT energy demand at with- drawal season, 1998-2002	40
2.18	Time series of natural gas price during withdrawal seasons from 1998 to 2002	41
2.19	ln Natural gas spot price vs. ERCOT energy demand at with- drawal season, 1998-2002, threshold \$4.3	41
2.20	ln Natural gas spot price vs. ERCOT energy demand at with- drawal season, 2003-2005	42

2.21	Time series of natural gas price during withdrawal seasons from 2003 to 2005	42
2.22	ln Natural gas spot price vs. ERCOT energy demand at withdrawal season, 2003-2005, threshold \$7.8	43
2.23	Average prices and threshold	43
3.1	Natural gas spot price of Henry Hub since 2000	52
3.2	Classic risk-return framework and the proposed risk-cost framework and their efficient frontiers and the iso-utility curves . . .	55
3.3	Interaction with markets	56
3.4	Two-regimes jump diffusion model of balancing energy prices .	66
3.5	Optimal natural gas portfolio	69
3.6	Optimal floating ratio at various volatilities	71
3.7	Comparison of outputs of the proposed framework for three months	72
4.1	Decomposition result of an original payout distribution	87
4.2	Maximum FSIs as a function of risk tolerance contrast ratio .	93
4.3	FSIs at different price jump probability	94
4.4	FSI of the aggregated IGFO contract	95
4.5	Aggregated ratio when replicating IGFO contracts	95
5.1	Traditional approach	101
5.2	Transition from traditional approach	103
5.3	Unified integrated risk management framework	104
5.4	Integrated risk management practice	105
5.5	Example of a framework	107

Chapter 1

Introduction

1.1 Background

For electric utility companies (EUCs), risk management has become a critical issue since the introduction of deregulation in US electricity markets. Before deregulation, EUCs enjoyed a regulated rate of return. Consequently, there were little, if any, incentives for the companies to manage their financial risk exposures since they were able to transfer the risks to their customers by charging them *ex post* surcharges. It was then no surprise to see that most of their operation and expansion strategies were centered around the cost minimization objective.

Electricity deregulation in the last decades has fundamentally changed the way EUCs operate as the rate of return is no longer guaranteed nor fixed, which implies that EUCs are solely responsible for their financial losses. EUCs now not only have the obligation to provide quality electricity service to their customers, but also need to take care of their own financial conditions in order to survive and grow in the markets. In other words, deregulation brings possible more opportunities for EUCs, but with risks.

The risks created by deregulation cannot be ignored or underestimated.

For example, real-time electricity prices, or so-called market clearing price of energy (MCPE), have exhibited tremendous volatilities in most, if not all the deregulated electricity markets. If an EUC has a generation forced outage and does not have adequate generation resources (either self-generation or arranged energy purchase), it has to rely on real-time balancing energy market to serve its demand, and could suffer from significant financial losses. In extreme case, EUCs could end up in bankruptcy simply because of such unexpected events, or risks.

Electricity deregulation calls for effective risk management for EUCs, which helps EUCs stay both operationally and financially healthy by hedging themselves against adverse events such as in the previous example. It could help maintain the revenue (returns) stability for EUCs and consequently could facilitate the growth of EUCs and better service to their customers. This dissertation presents models for several key factors in deregulated electricity markets and proposes some novel frameworks in the integrated risk management for EUCs.

1.2 Literature Review

Integrated risk management in general involves managing various kinds of risks such as volumetric risks, price risks, physical supply/delivery risk, operational risks, and financial risk, etc. In this section, we review some of the literature that has been dedicated to the various aspects of the integrated risk management framework for the deregulated electricity markets.

Risk Management for EUC

Cabero *et al* [22] proposed an integrated risk management model using a coherent risk measure, namely Conditional Value at Risk, or CVaR, to optimize a hydrothermal generation company's decision. Mo *et al* [73] proposed an integrated risk management framework for managing revenue risk by integrating the load scheduling and contract management. Ni *et al* [74] presented an optimization based algorithm to provide efficient energy and reserve offering strategies for a hydrothermal power system. The objective function is to maximize expected profit while including a penalty for price variance. Albuyeh and Kumar [5] provided an overview of the decision support tools that are essential to the deregulated wholesale electricity market participants. It recognizes the importance of system integration of generation management, data management to trade managements, etc.

Deregulated Electricity Markets Analysis

Hesmondhalgh [49] reviewed the New Electricity Trading Arrangements (NETA) in England and Wales. NETA is a decentralized electricity mechanism, which treats electricity as far as possible like any other commodities. It shows the positive changes happened in the market and compares the advantages of NETA with other centralized electricity market. Denton *et al* [33] described the market risks exposures to EUC in the deregulated electricity markets. The risks are first categorized in terms of time frame, and then by nature. Different optimization objectives are described for different time frames. The needs for integration of various risks are addressed. The authors

pointed out drawbacks of some optimization methods and assumptions, as well the difficulties faced by practitioners. They highlighted the use of expected profit maximization strategy in short-term planning as well the use of utility maximization objective and various risk metrics for mid-term and long-term planning.

Risk Analysis Methodology

Linares [69] proposed a framework to deal with multiple criteria decision making for power system planning. First various characteristics of available technologies and fuels are used to generate scenarios. Then risk preferences of various decision makers are modeled, as well as a consensus one. After selecting the best strategy for every decision maker and the consensus one, these strategies are tested against other decision makers' risk preference and the optimal one is the one that best compromises over all risk preferences. Linares also mentioned that the deterministic method and the probabilistic method are not favorable methods in dealing with uncertainties in system planning. Miranda and Proenca [72] compared the traditional probabilistic choice (PC) methodology and the risk analysis (RA) approach in system planning. The conclusion is that probabilistic choice tends to ignore compromised solutions and produce more risky projects. PC can be used if and only if the applied subject can be assumed to have a high repetition in the planning life span, otherwise RA should be performed. Miranda and Proenca also identified that PC is not convenient in electricity system planning as it tends to ignore compromise solutions and produce riskier results, while RA is a better choice [71].

Hedging in Electricity Markets

Gabriel *et al* [41] provided an analysis on the electricity retailer's settlement risk by using different load forecast strategies. Chung *et al* [27] presented analysis of forward contract with bilateral options as a new risk management product in deregulated electricity markets. This type of contract provides both the seller and the buyer of the forward contract the options to reject providing or receiving the energy. Tanlapco *et al* [96] described a risk minimization hedging strategy using futures contracts. Optimal hedging ratio, as well two strategies, namely direct hedging and cross hedging, are discussed. The optimization is based on risk minimization since they assume a very risky environment, in which case the utility maximization problem may simply collapse to risk minimization. Brown and Burke [20] analyzes the concept of performance based rates (PBR), which starts with the electricity market deregulations. It proposes a revised sequential Monte Carlo simulation to evaluate the system-wide component failure rate. Utility companies can use this framework to analyze potential PBR risks and re-negotiate the PBR contract if the result is unfavorable. Yet no specific criterion is mentioned on how EUC determines whether it needs to re-negotiate a PBR contract. Gedra [42] reviewed the properties of callable forward contracts, as well as puttable forward contracts and the optimal selection strategy of contracts by market participants. Collins [28] analyzed the economics of electricity hedging in the early California electricity market. Hedging using NYMEX futures contracts is shown to pose potentially wide basis risk and a change to use physical futures price index,

i.e. California-Oregon Boarder (COB) price index, is proposed.

Resource Planning/Scheduling Implementation

Crousillat *et al* [29] realized that there are conflicting objectives and risk in power system planning. The authors recommend that these conflicts need to be analyzed, quantified and hedged. Siddiqi [88] applied the real option analysis developed by Smith and Nau [92] in long term project evaluation and integrated resource planning. Yamin and Shahidepour [103] presented a risk based self-scheduling strategy for generation companies. Probabilities of reserves to be called are assigned in risk analysis. Das and Wollenberg [32] presented a simulation process to evaluate the financial risks of generation forced outage after bidding is accepted by ISO for multiple generators using Value at Risk, or VaR, as a risk measure. Dahlgren *et al* [30] summarized the applications of risk assessment in energy trading. These assessments include VaR, CVaR and hedging. Examples are given to demonstrate these applications. Douglas *et al* [34] presented a methodology in assessing the short term load forecast risk. The risk is due to the weather forecast errors and the short term load forecasting (STLF) model errors and price uncertainty is not included. Therefore, it addresses the volumetric risk. Bjorgan *et al* [13] utilized modern utility theory in the contract evaluation process. It considers the alternative between futures contracts and spot markets as one hedging option and self-production as the other. Fuel constraint is considered in the modeling of the self-production approach. Sheble [86] presented a decision analysis tool with assigned subjective probabilities for GENCO dispatchers. It realizes the

importance of integrating certain business objective in the decision making process in order to stay competitive in the electricity markets. Andrews [6] studied different strategies for managing risks in resource planning and compares various risk analysis techniques. Flexibility and robustness were identified as the two general classes of proactive technical risk management strategies.

Power Systems Risk Analysis

Popovic and Popovic [79] proposed a fuzzy logic system for supply restoration in the system fault risk management of the distribution network. The goal is to determine an optimal restoration network that provides a minimal total expected cost of undelivered energy during the restoration. Dai *et al* [31] proposed a sequential mean variance (SMV) model to evaluate the power system reliability over a mid-term planning period using a risk index, which is the expected monetary impact. Lian and Billinton [68] described a composite system operating reserve risk assessment. It includes the dependent events associated with common mode and station originated outages in the analysis. But it is just a risk analysis methodology and does not deal with the risk. Fu *et al* [40] presented a generic procedure to evaluate the outage risks of the special protection systems (SPS). No specific decision making rule is proposed. Fu *et al* [39] also presented a generic procedure to evaluate the outage risks of transformer thermal loading capacity. No specific decision making rule is proposed. Billinton and Chen [12] presented two risk based capacity benefit factors in wind energy conversion systems (WECS) which are believed to be able to help system planners and utility managers to access the capacity worth

of WECS.

1.3 Motivation

This dissertation addresses the following aspects of the integrated risk management for EUCs in deregulated electricity markets. The major contributions are three-fold: *market fundamental analysis*, *integrated supply optimization* and *risk management practice*. They are further discussed as follows.

1.3.1 Market Fundamental Analysis

In deregulated electricity markets, electricity demand and price are the two most important fundamental factors as they used to and should be. People have recognized that it is important to be able to produce accurate forecasts of these two factors, but some of the important aspects of modeling and forecasting these two factors often are ignored.

An accurate STLF system is highly critical in the integrated risk management for an EUC. Basically almost all the short term operation decisions such as unit commitment and electricity purchases are based on the daily load forecasts. Various techniques have been developed and applied in STLF. However, no literature has been dedicated to the special area of weather sensitive load. In fact, some of the techniques actually perform the worst at extreme weather, when the balancing energy prices could be extreme, and therefore fail to meet the purpose of STLF. The adverse consequences of bad STLF in extreme weather could range from tremendous financial losses to blackouts such

as during the most recent rolling black out in ERCOT area in April 17th, 2006. We are motivated to proposed a knowledge based generic STLF framework to tackle this problem and it has been integrated into the energy management system (EMS) of the Lower Colorado Rive Authority.

Wholesale electricity price forecast has been the core piece of the evaluation of various transaction and electricity products. The traditional forecasting techniques are focused on curve fitting without taking into account of the unique supply/demand relationship in power systems. As a result, the accuracy is limited. In the electricity price model proposed in this dissertation, we use the empirical findings to unveil the two key factors behind the electricity price dynamics and therefore improve the accuracy and explanatory power of the model.

Another aspect of the research is to study the potential correlation between the market fundamentals. In most ISO regions, natural gas is the fuel of the marginal units and therefore the electricity prices are deemed a multiple (marginal heat rate, or MHR) of the natural gas prices. Since MHR is widely believed to be driven by electricity load, it is modeled separately from natural gas price in common practice. However, is this assumption of independence between electricity demand and natural gas prices always true? Our study in ERCOT region shows that it depends.

1.3.2 Integrated Supply Optimization

Managing the fuel supply (mainly natural gas) in deregulated electricity markets is more challenging than ever before. Traditionally this problem was focused on operational aspects and most literature targeted at cost minimization. This could cause serious problems for EUCs as electricity markets move into the deregulated era. First, a riskier strategy is more likely to be adopted using traditional cost minimization framework [72]. Secondly, natural gas price volatility was not taken into account in the modeling, not to mention electricity price modeling. Finally, the risk preferences of the management team was left out. An EUC needs an integrated supply optimization framework to solve these problems.

The proposed natural gas supply optimization framework is based on utility theory, which is fundamental to modern management science. The framework integrates the risk preferences of the management team, the physical consumption and constraints of the power plants, the financial aspects of the various energy fundamental factors including price forecasts of natural gas and electricity, as well as various other factors. Although we only show an application of monthly natural gas supply optimization, this framework can be easily extended to address different time span. An extra feature of this framework is to be able to serve as a benchmarking tool for a trader's performance.

The study presented in this dissertation is considered the first integrated supply optimization framework in the deregulated electricity markets.

1.3.3 Risk Management Practice

Using various financial hedging tools is now common practice for EUCs in deregulated electricity markets. Insurance on generation forced outages (IGFO) is one of the novel financial products.

The focus of our study is on determine the feasible structures of an IGFO in our research. This is important as an ill-structured IGFO could turn out to be infeasible and waste both time and money of the two counter parties. The study also shows that the proposed framework is able to help EUCs identify better counter parties and strategies in terms of feasible structures.

In our application, we apply utility theory to identify the feasibility structures of an IGFO contract. Impacts on the IGFO feasibility from factors such as risk preference contrast ratio and probability of price jumps, as well EUC's decision to combine two IGFO contracts, are studied.

1.4 Dissertation Organization

Chapter 2 discusses two modeling studies, including a short-term load forecasting (STLF) model for weather sensitive load and a study of day-ahead spot electricity price dynamics. The studies detail the integration of weather segmentation into statistical STLF modeling efforts and identify the impact of system-wide generation forced outage in day-ahead electricity spot price dynamics. A study on the correlation between natural gas spot price and electricity demand in the ERCOT region is also presented.

In Chapter 3, we develop a risk management framework for EUCs who own and operate natural gas fired power plants (NGFPP). As NGFPPs have become a major source of electricity generation in the United States, it is critical for EUCs to optimize their fuel purchase strategy. Electricity deregulation has brought significant risk exposures to NGFPP owners and operators. The major contribution of the framework is to achieve the goal of cost-risk balance in the purchase of natural gas, which the traditional cost-minimization framework did not consider.

Chapter 4 proposes an evaluation methodology for EUCs to identify the feasible structures of insurance on generation forced outages (IGFO). IGFO is usually a bilateral contract between an insurance company (insurer) who underwrites the contract and an EUC (insured) who owns the generation. The difference in risk aversion of each party determines the feasible structures of an IGFO. We propose a feasible structure index, or FSI, which is the spread between the maximum price that the insured is willing to pay and the minimum price that the insurer is willing to sell, to help determine the optimal IGFO structure. Our study provides a framework for calculating FSI and explores how it could be affected by various factors and behaviors. The study is important since not every IGFO structure is feasible.

In Chapter 5, we first summarize the research presented in this dissertation. We then discuss the transition from traditional cost minimization framework to the proposed integrated risk management framework. Finally, we discuss the possible future research.

Chapter 2

Modeling the Fundamentals in Deregulated Electricity Market

Load and price are two basic building blocks in the power system economics and energy finance areas. Electric load, with some exception of load as resource (LAR), should be independent of electricity market design. Yet electricity price, while in some degree has to do with the market design, is still fundamentally driven by the unique requirement of real-time supply and demand balance of the power systems. A thorough understanding of these fundamental drivers is a foundation of the integrated risk management framework presented later in the dissertation.

This section first describes a short-term load forecasting (STLF) model as short term load forecasting has long been an interesting research topic because most power systems activities including daily system planning are based on electricity load prediction. Then we put forth some empirical studies on day-ahead electricity spot price dynamics. Finally, we studied the correlation between the fuel (natural gas) price and electricity demand in ERCOT.

Section 2.1 discusses some current modeling methods and presents a forecasting model for weather sensitive load with integration of weather seg-

mentations. Section 2.2 studies the day-ahead electricity spot price dynamics. The observations identify system-wide load level as one major driver in the dynamics and system-wide generation forced outage as another key driver. Section 2.3 studies the correlation between the natural gas spot price and the electricity demand in ERCOT region. We find marked correlation exists under certain situations.

2.1 STLF using Knowledge Based ARX Models

STLF provides electricity load forecast with lead times from minutes to weeks. An accurate STLF system is essential to the energy management systems (EMS) of any EUC. STLF has never been easy because of the complexity of electricity load. It not only exhibits the time-series effect, but also is affected by many exogenous variables, especially weather variables.

Various models and techniques have been developed in this area. Generally speaking, there are two major approaches. The first or traditional approach is based on statistical models such as time-series analysis and causal models [46], [78], [98] and [37]. Another approach uses artificial intelligence models including artificial neural networks (ANN) [70], [26], [76], [80], [81], [77], [97], [61] and [82].

In recent decades, ANN has received a great deal of attention in STLF applications. However, concerns regarding issues of design, implementation, and validation of ANN models still remain unclear [51] and [1]. Moreover, most, if not all, of the research is applied to electricity load that is relatively

stable and has no frequent or rapid variation.

For weather-sensitive electricity load, dramatic variation may occur due to weather events such as cold fronts or heat waves. A good example is residential loads that can increase significantly due to the heating demands when a cold front occurs. In such cases, the advantage of the ANN model's robustness may adversely impact its performance because it may treat such weather changes as outliers and tend to minimize their effects by smoothing out the outputs [77]. This may lead to under-forecasting when such weather events happen and over-forecasting after that. With the black-box like structure of ANN models, very little insight about how the model responds to such events can be gained, even for the model developers. Therefore, people have to either accept the output or reject it [75].

On the other hand, traditional approaches have the advantage of clear physical interpretations and are able to quickly respond to changes of variables. The impact of any input variable to the electricity load and the time-series effect can be easily found by reviewing the models. Such approaches may provide limited accuracy because of the use of a typical approach in which only a single model is developed to model electricity load.

We propose an implementation of traditional approaches by performing knowledge-based weather segmentations and utilizing auto-regression with exogenous variables (ARX) models. This method not only has clear physical interpretations that ANN models lack, but it is also able to provide better forecasts than what we will refer to as typical approaches (TA), which use a

single statistical model to forecast electricity load and does not distinguish weather segmentation.

2.1.1 Knowledge-Based Weather Segmentations

Weather variables are the most important factors in modeling weather-sensitive electricity load. Reference [81] has classified weather patterns into the following four major patterns:

1. Normal Days: steady weather, hot in summer or cold in winter
2. Abnormal Days: days with irregular weather such as cool days in summer or warm days in winter
3. Extreme Days: very hot summer days or very cold winter days
4. Transition Days: warm spring days or cold fall days, interpreted as the beginning of summer or winter, respectively

These segmentations are mostly region-dependent and require that load forecasters have knowledge of and experience with local weather patterns. This process may also involve statistical analysis of historical weather data.

In our approach, instead of building a single model for all these patterns, one ARX model is developed for each pattern in order to directly model the impact of weather changes on electricity load. Such impacts are quite different for each weather pattern. Incorporating the concept of knowledge-based

weather segmentations into our forecasting models enables us to utilize multiple ARX models that are individually linear in nature to correctly identify and sufficiently model the non-linear impact of weather changes on electricity load.

2.1.2 Scheme for Model Development and Application

The scheme for developing a forecasting system model is shown in Figure 2.1. In this scheme, outliers in historical data are first excluded to obtain the clean data for model estimation. Then the data are separated into individual weather event categories for developing the individual part of the ARX model. Finally, a complete knowledge-based ARX model can be obtained by aggregating the three individual parts.

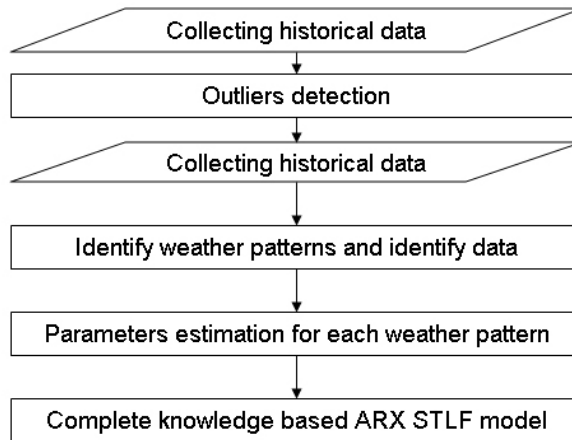


Figure 2.1: Scheme of Developing Forecasting System.

Figure 2.2 shows the scheme for applying the forecasting system. At first, all necessary next-day weather forecasts such as temperature and satel-

lite images are used to determine the pattern of the next day. After that, a corresponding part of the ARX model is chosen to produce a final load forecast.

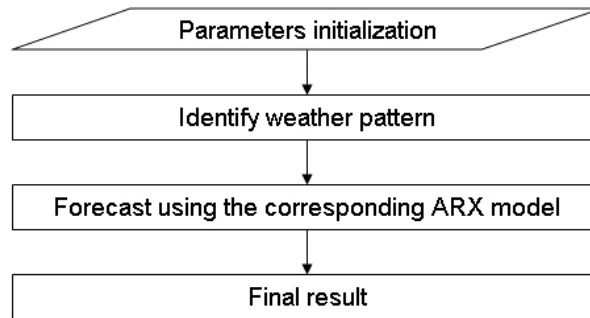


Figure 2.2: Scheme of Applying Forecasting System.

2.1.3 Application

The proposed model has been used to produce winter next-day electricity load forecasting in central Texas area, where most of the load is residential, for two testing periods in 2/10/04-2/16/04 and 2/22/04-2/28/04. The peak load during the cold front increased by close to 100% compared to the peak load for a normal day.

Two weather patterns are defined besides normal winter day pattern. They are type I cold front day and type II cold front day, defined as follows. Professional weather services, which provide hourly forecasts of weather parameters such as temperature and humidity, can be purchased by EUCs to identify these patterns.

1. Type I cold front days: winter days with a very cold morning and quick

warm-up later

2. Type II cold front days: winter days with the temperatures remaining almost flat throughout the day

Three test benchmarks are chosen to compare results:

1. Daily Mean Absolute Percentage Error (DMAPE)

$$DMAPE = \sum \left| \frac{p_i - \hat{p}_i}{p_i} \right| / 24 \quad (2.1)$$

where

\hat{p}_i : the value of forecasted electricity load;

p_i : the value of actual load.

2. Standard Deviation (St. Dev.) of forecast errors
3. Daily Absolute Maximum Percentage Error (DAMPE)

$$DAMPE = |p_t - \hat{p}_t| / p_t \quad (2.2)$$

where t : the time such that $|p_t - \hat{p}_t| = \max |p_i - \hat{p}_i|, i=1, 2, \dots, 24$.

First Test Week

Figure 2.3 shows the next-day load forecast results from both the proposed model and the TA for the week of 02/10/04-02/16/04, along with the actual load curves.

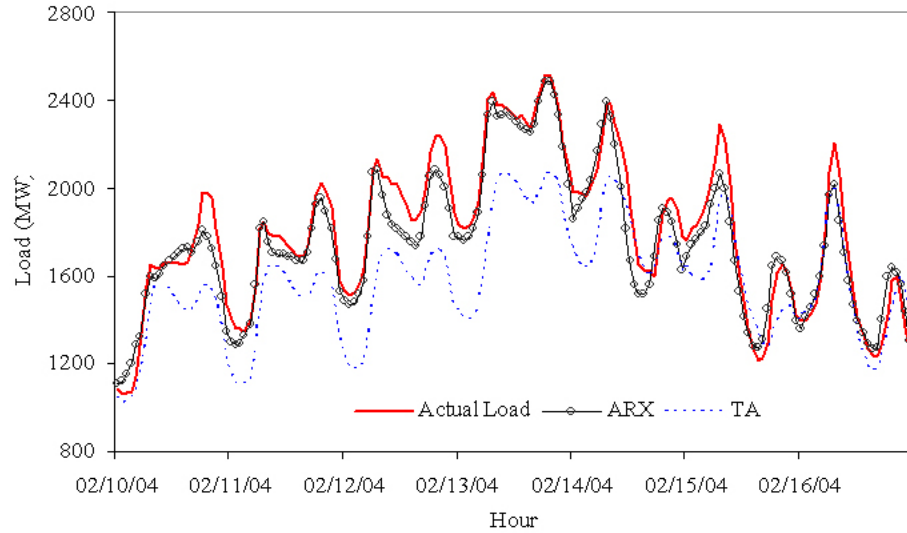


Figure 2.3: Forecast Comparisons for the First Test Week

Table 2.1 shows the DMAPE, the St. Dev. and the DAMPE for both ARX and TA. The comparison indicates that ARX performs better than TA most of the time.

		02/10/04	02/11/04	02/12/04	02/13/04	02/14/04	02/15/04	02/16/04
Day Type		Type II	Type II	Type II	Type II	Normal	Type I	Type I
DMAPE	ARX	5.4%	2.9%	5.6%	1.8%	5.4%	5.0%	4.3%
	TA	11.6%	15.4%	20.8%	18.0%	9.4%	9.7%	5.6%
St. Dev.	ARX	6.7%	2.0%	2.7%	0.8%	5.6%	5.9%	5.4%
	TA	6.4%	4.8%	4.6%	4.8%	6.6%	9.4%	5.8%
DAMPE	ARX	11.8%	5.4%	10.0%	3.0%	12.3%	9.8%	10.0%
	TA	21.9%	20.2%	30.2%	27.4%	15.7%	19.5%	9.3%

Table 2.1: Comparisons of Both Models for the First Test Week

Second Test Week

Figure 2.4 shows the comparison of two forecasts with actual load for the week of 02/22/04 - 02/28/04.

Table 2.2 indicates that the proposed model performs better most of

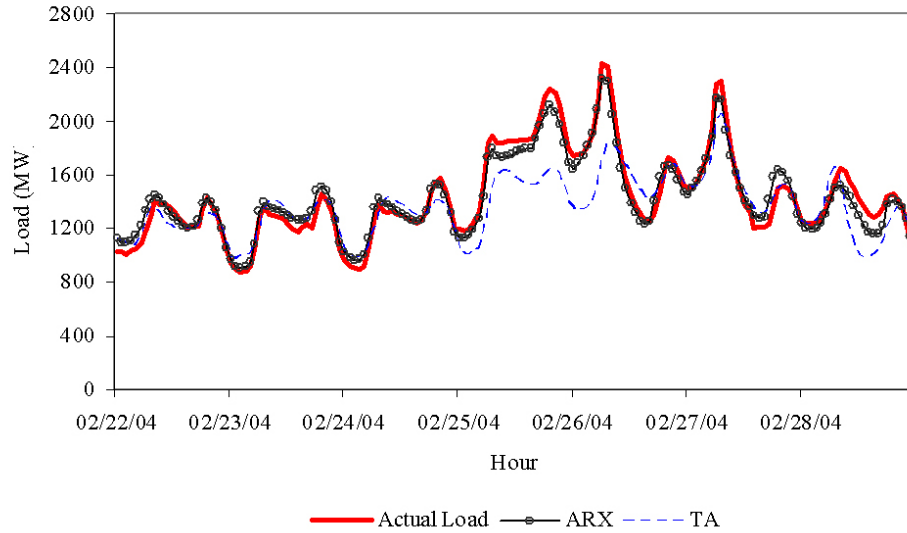


Figure 2.4: Forecast Comparisons for the Second Test Week

the time.

		02/22/04	02/23/04	02/24/04	02/25/04	02/26/04	02/27/04	02/28/04
Day Type		Normal	Normal	Normal	Type II	Type I	Type I	Normal
DMAPE	ARX	4.6%	4.8%	3.5%	4.7%	3.7%	4.5%	5.5%
	TA	5.4%	6.6%	6.5%	19.1%	13.6%	5.2%	12.0%
St. Dev.	ARX	4.9%	2.1%	3.7%	1.1%	3.7%	5.8%	4.1%
	TA	6.1%	4.8%	7.0%	5.2%	15.7%	6.6%	12.9%
DAMPE	ARX	13.7%	10.1%	9.4%	6.5%	4.9%	14.8%	11.0%
	TA	8.8%	9.9%	10.8%	27.1%	30.0%	12.9%	28.5%

Table 2.2: Comparisons of Both Models for the Second Test Week

Summary

A summary of comparisons for the two testing weeks is presented in Table 2.3. The summary shows a significant improvement of the proposed model over TA.

Comparison with ANN models

For the second test week, we also use a set of commercial ANN software

		2/9/2004 - 2/16/04	2/22/2004 - 2/28/04
Weekly MAPE	ARX	4.4%	4.5%
	TA	12.9%	9.8%
St. Dev.	ARX	4.9%	5.4%
	TA	8.6%	11.9%

Table 2.3: WMAPE and Standard Deviation for Both Weeks

which uses the same set of training data to perform a forecast. The software forecasts the total energy and profiles it using forecasted hourly weights. The forecast by ANN are compared to those of the proposed model and TA. The results of daily MAPE and Weekly MAPE are shown in Table 2.4. It shows that while the proposed model produces slightly worse forecasts than ANN during normal days, it produces significantly better forecasts in abnormal weather situations. Therefore, introducing knowledge-based weather segmentation has significantly improved the overall performance of our load forecasting models (4.5% WMAPE compared to 7.3%). We also believe that if knowledge-based weather segmentation concept is integrated into ANN modeling, its accuracy may also be improved, but the ANN model structure for each weather pattern will still remain a black-box.

	02/22/04	02/23/04	02/24/04	02/25/04	02/26/04	02/27/04	02/28/04	
Day Type	Normal	Normal	Normal	Type II	Type I	Type I	Normal	WMAPE
ARX	4.6%	4.8%	3.5%	4.7%	3.7%	4.5%	5.5%	4.5%
ANN	2.4%	4.4%	4.7%	8.4%	13.1%	14.4%	3.6%	7.3%
TA	5.4%	6.6%	6.5%	19.1%	13.6%	5.2%	12.0%	9.8%

Table 2.4: DAMPE and WMAPE of All Models for the Second Test Week

2.2 Electricity Price Dynamics

Modeling electricity spot market price is important for valuation of financial transactions in competitive electricity markets. In the deregulated electricity market, spot price of electricity can be affected by certain predictable economic factors such as system-wide capacity level, load level, or generation outages. Therefore, simple curve-fitting models without consideration of the important economic factors sometimes do not perform well and can be improved [65] and [52].

We studied the impacts of two key factors on electricity spot market price dynamics: system-wide load-capacity ratio and system-wide generation forced outages and propose a multivariate electricity spot market price model.

2.2.1 Suggestions of Economic Research

Economic research has been carried out intensively to understand electricity spot market price dynamics in both economic dispatch, such as summarized in [94], [101], and strategic behavior, as in [64], [43], [18], [17], [19], [83], [104], [9] and [62].

An important common conclusion from previous economic research is that the system-wide generation capacity constraint level plays a critical role in the electricity spot market price dynamics, especially price spikes. The constraint level is mainly determined by two factors: system-wide load level and system-wide generation outage level. In the electricity market, higher load indicates higher demand, higher generation outages indicate reduced supply,

and both factors can affect the market supply-demand condition immediately. Figure 2.5 illustrates this conclusion.

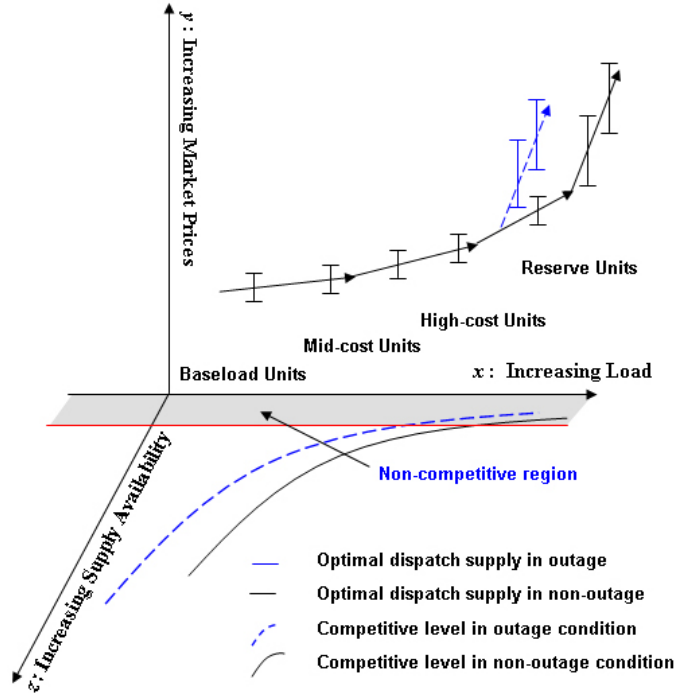


Figure 2.5: Dynamic Evolution of the Electricity Spot Market Price

Studies of economic dispatch suggest that generation should be deployed in the ascending order of marginal production costs. Consequently, both marginal production costs of electricity and market prices should increase as load increases. Furthermore, high load with lower probability and emergency generation are usually supplied by only a few less frequently used, less efficient and higher production cost reserve generations. Therefore, the electricity price jumps when the reserve generations are deployed as marginal units.

Market competitions could deteriorate or even disappear as the load and constraint levels increase. Research suggests that when the number of competitors is small, strategic behaviors could be triggered [64], [43]. Consequently, market price could be driven further above the actual marginal production cost. The gray area in the x-z plane represents such a non-competitive region, where only few competitors exist. The blue curves show the impact of generation outages on the shape of the *z-shape* curve and the level of supply availability.

2.2.2 Empirical Investigation Results

This section presents an empirical investigation in the ERCOT market on the impacts of system-wide load-capacity ratio (SLCR) and system-wide generation forced outages (SGFO) on the electricity spot market price dynamics. The electricity spot market prices used herein are wholesale day-ahead on-peak electricity prices in 1999 (June-September), published in Megawatt Daily.

Definition 2.1: System Load Capacity Ratio (SLCR)

$$SLCR = \text{Systemwide Peak Load} / \text{Systemwide Planned Capacity}$$

SLCR is a better system-wide generation capacity constraint level index than the peak load because the value of peak load by itself cannot truly reflect the capacity constraint level. With the ERCOT market, for example, a 42

GW peak load by itself does not contain any information on its impact on the constraint level. It would have been an extremely high load when total generation capacity was only 43 GW at 15 years ago. Nowadays, however, it is considered a low load as total generation capacity is over 75 GW. When comparing the corresponding SLCR of the 42 GW peak load, it was over 97% at 15 years ago and 56% now. Apparently, SLCR better represents the capacity constraint level.

The percentage of available capacity when the peak load occurs can also be easily calculated using SLCR. For example, 90% SLCR indicates that 90% of system-wide planned capacity has been deployed in order to meet the peak load demand, and only 10% is left for contingency.

In ERCOT market, the reliability requirement of power systems requires an approximate 12.5% reserve margin [36], which implies that 88.9% SLCR is the threshold alone which some reserves could start being called upon for service. As we have pointed out, price jumps are then possible even without market manipulation due to the utilization of older, less efficient power plants.

Definition 2.2: System wide Generation Forced Outages (SGFO)

SGFO = The System Wide Aggregated Generation Outage Capacity Amount

SGFO data generally is confidential information in the competitive environment. We estimate SGFO data using generation emission records collected and published by the Environmental Protection Agency (EPA) [59].

Observation 2.2.A: Existence of the Price Jumps Threshold

Figure 2.6 shows the existence of a price jump threshold. When system-wide peak load level, or SLCR, passes the threshold, price jumps may occur. The observation is in accordance with the *z-shape* curve shown in Figure 2.5.

We introduce the market supply curve, as shown in Figure 2.6(a). Each point in the curve represents a pair of price (\$/MWh, y-axis) and the corresponding system-wide peak load (MW, x-axis). The prices-load relationship is complicated in Figure 2.6(a).

We define two load regions (high/low-load) using a 46 GW threshold and then plot the market supply curve in each load region in Figure 2.6(b, c), making the price-load relation clearer. Figure 2.6(b) shows that price fluctuates around \$30 in the low-load region and starts dispersing as load increases. Figure 2.6(c) shows that price suddenly becomes very volatile in the high-load region and jumps over a very wide range. (note that the price axes have very different scales in Figure 2.6(b) and Figure 2.6(c))

Observation 2.2.B: Price Impact of SGFO

Figure 2.7 shows that the impact of SGFO on the electricity spot market prices becomes effective in a high-SLCR or high-load region.

Using estimated daily SGFO data, we plot the time series of electricity spot market prices (\$/MWh, gray-bar), ERCOT system-wide peak demand (MW, blue-curve), and SGFO data (MW, red-curve) in Figure 2.7(a), where the prices-SGFO relation is unclear. However, when we plot the time series of

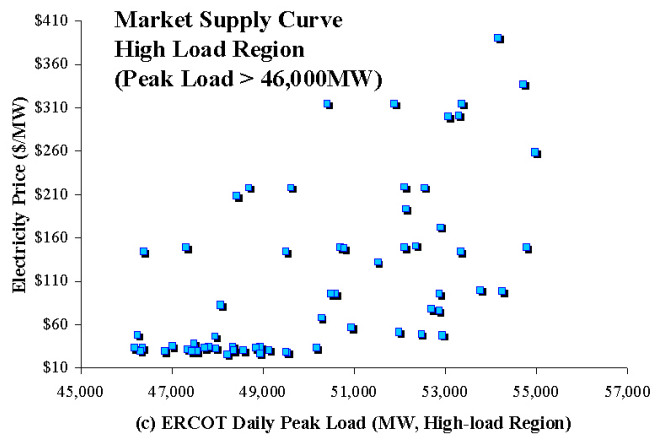
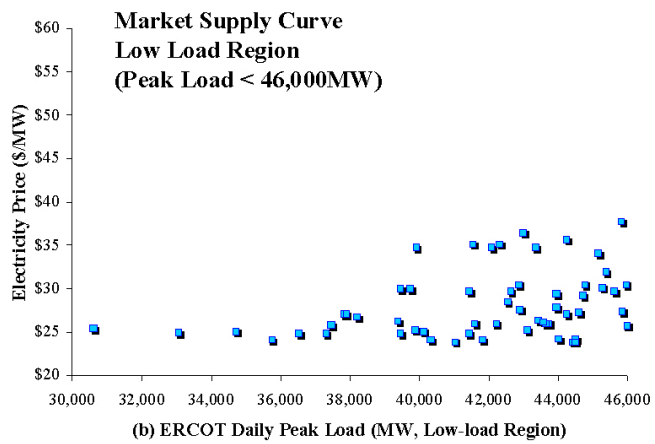
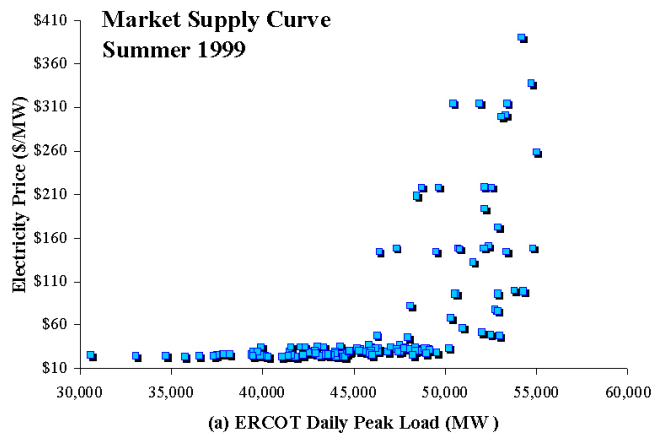
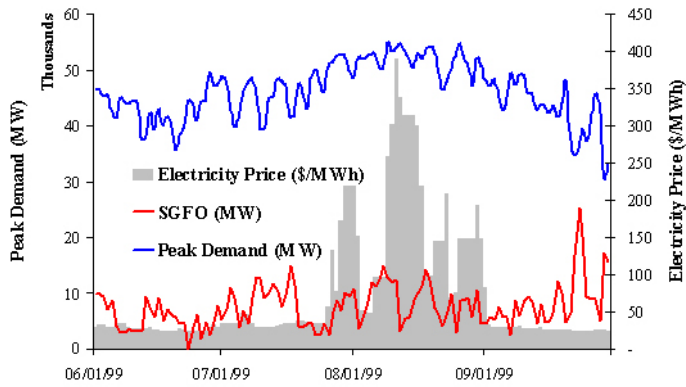
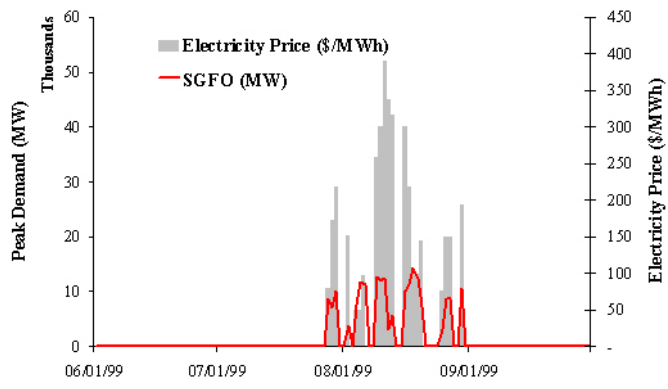


Figure 2.6: Existence of Price Jump Threshold



(a) Time Series of market demand, GFO capacity and price



(b) Time Series of market demand, GFO capacity and price at high-load region

Figure 2.7: Time series of market demand, GFO capacity and price index

price and SGFO data at above a 52 GW load, as in Figure 2.7(b), the impact of SGFO on the electricity spot market prices becomes clear: price jumps are highly correlated with SGFO in this high-load region. The 52 GW load threshold in 1999 corresponds to an SLCR of 90% which is considerably high.

Observation 2.2.C: SLCR and SGFO in Price Dynamics

We show that system-wide peak load or SLCR is the dominant factor in the electricity spot market price dynamics and SGFO only takes effect in the high-load/SLCR region in Figure 2.8. In the yellow window, which represents the low-load/SLCR region, the impact of SFGO is insignificant. The patterns of two sets of price-load pairs (marked with blue dots and red dots respectively), with or without significant SGFO, are almost identical. In the blue window, which represents the high-load/SLCR region, most price spikes occur when SGFO is significant, represented with the blue dots.

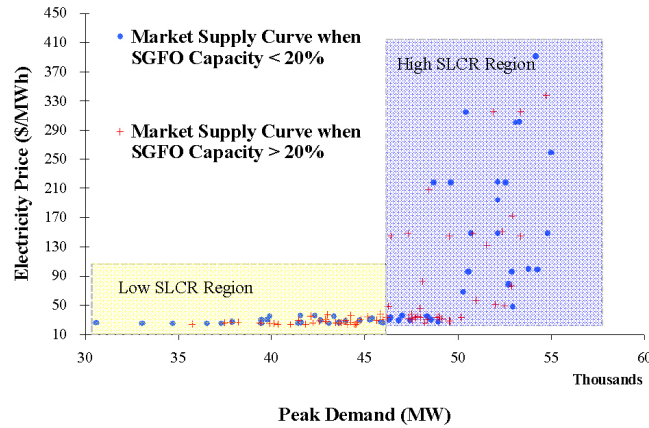


Figure 2.8: SLCR and SGFO in the Price Dynamics

Figure 2.8 plots market supply curves based on different *SLCR* and *SGFO* levels. We use high/low-load regions with the 46 GW cutoff load defined in Observation A to reflect *SLCR* levels according to Definition 2.1. The corresponding *SLCR* of the 46 GW load is 80%. The market supply curve of the high-*SLCR* region is contained in the blue window, and that of the low-*SLCR* region is contained in the yellow window.

We also define two *SGFO* levels (high/low): a high-*SGFO* region for days where *SGFO* capacity is more than 20% of the total considered capacity, and a low-*SGFO* region for the rest. The market supply curve in the high-*SGFO* region consists of all red crosses; that of the low-*SGFO* region consists of all blue dots.

The price gradually increases with low volatility in the low-*SLCR* region regardless of *SGFO* levels. Several high-*SGFO* days do occur in this region, but have not caused price jumps. On the other hand, the prices exhibit extremely high volatility in the high-*SLCR* region, also regardless of *SGFO* levels. In fact, in the high-load region, about 31% of high-*SGFO* days are associated with price jumps over \$210, while less than 9% of low-*SGFO* days are associated with such price jumps.

2.2.3 Observations Summary

1. *SLCR*, or peak load, reflects the maximum market demand level. There exists an *SLCR* threshold dividing low load/low price volatility region and high load/high volatility region.

2. *SGFO* reflects market supply availability. Its impact on price is less significant in the low-load region, while its impact becomes significant in the high load region, where the price is sensitive to system generation outages.

2.3 Correlation between HSC Natural Gas Spot Price and ERCOT Electricity Demand

Natural gas fired power plants, or NGFPPs, are usually used as the peaking units in electricity markets and, in competitive electricity markets, the on-peak electricity spot price are usually set based on the marginal production cost of NGFPPs. Because of the engineering characteristics of NGFPP, the marginal production cost of NGFPPs, or electricity price P , is usually modeled as follows:

$$P = MHR \times P_{ng} \quad (2.3)$$

where

MHR : marginal generation heat rate of NGFPPs,

P_{ng} : the natural gas spot price.

One common practice in modeling electricity spot prices is to treat MHR and P_{ng} as independent variables and model them separately before multiplying them to produce the spot price [3]. Such assumption is intuitive as it reflects the engineering characteristics of NGFPPs and makes it easier for modeling effort. However, such assumption needs to be validated since

the natural gas spot price is determined by supply-demand of natural gas and electricity demand, as part of the natural gas consumption, could (and should) potentially affect the supply-demand in natural gas and consequently affect P_{ng} .

In this section, we study the relationship between the electricity demand in ERCOT and the natural gas spot prices (cash price). This will provide helpful information on the validity of the modeling in [23]. Also this analysis serves as a caveat to the modeling efforts in other ISO regions.

2.3.1 Data Description

Natural gas spot price data used in this section are the Houston Ship Channel (HSC) data collected by Gas Daily, a publication by Platts. HSC is a major natural gas distribution hub in Texas and the cash price is for next day delivery. We used the natural logarithm (\ln) of the price in the calculation as the price movement has been widely believed to be log normal [85].

The electricity data used are the aggregated daily electricity energy consumption in ERCOT region, collected and published by Global Energy. All data are from January 1st 1998 to December 31st, 2005.

2.3.2 Overall Analysis

The results of this section are shown in Figure 2.9 through Figure 2.12.

Figure 2.9 shows the time series of ERCOT daily electricity consumptions and the natural gas spot prices. As we can see, the year of 2003 is the

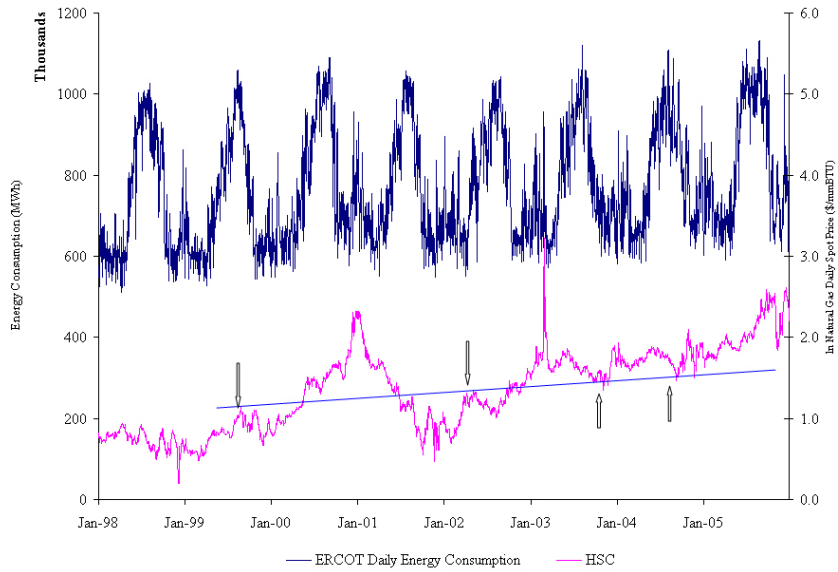


Figure 2.9: ERCOT Daily Consumptions and Natural Gas Spot Prices

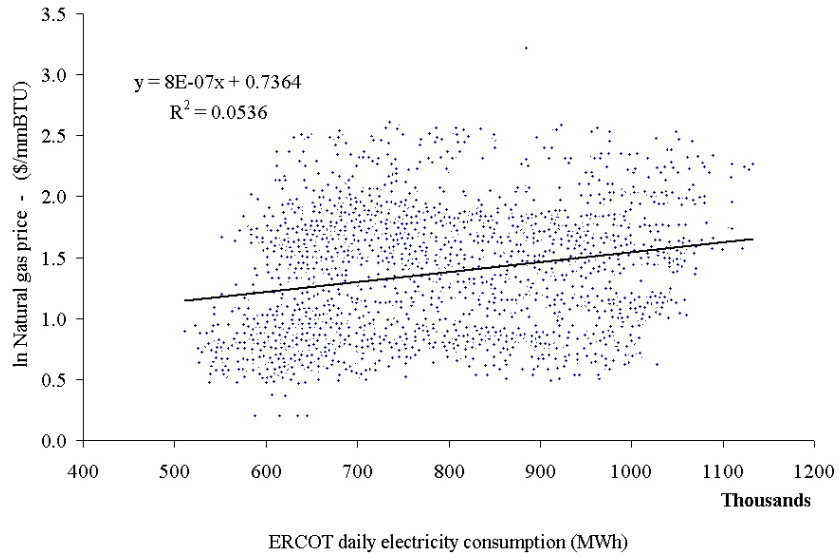


Figure 2.10: ERCOT daily electricity consumption vs. ln natural gas daily spot price from 1998 to 2005

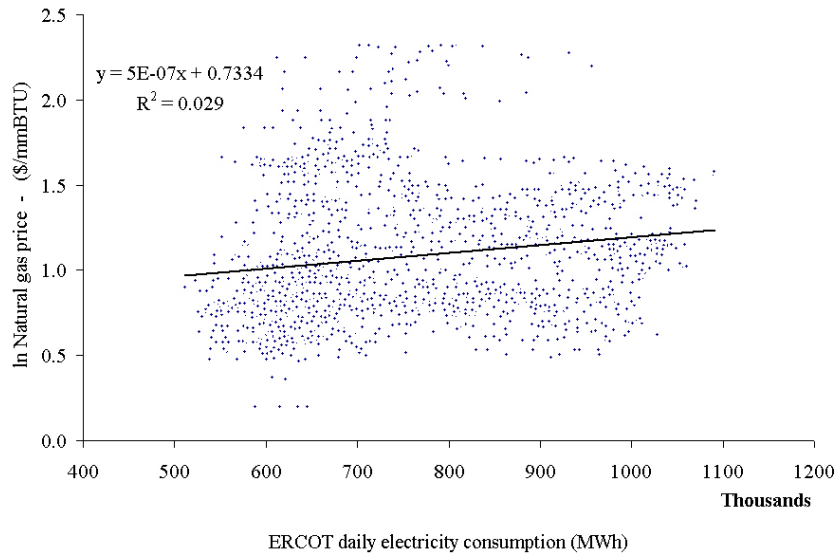


Figure 2.11: ERCOT daily electricity consumption vs. ln natural gas daily spot price from 1998 to 2002

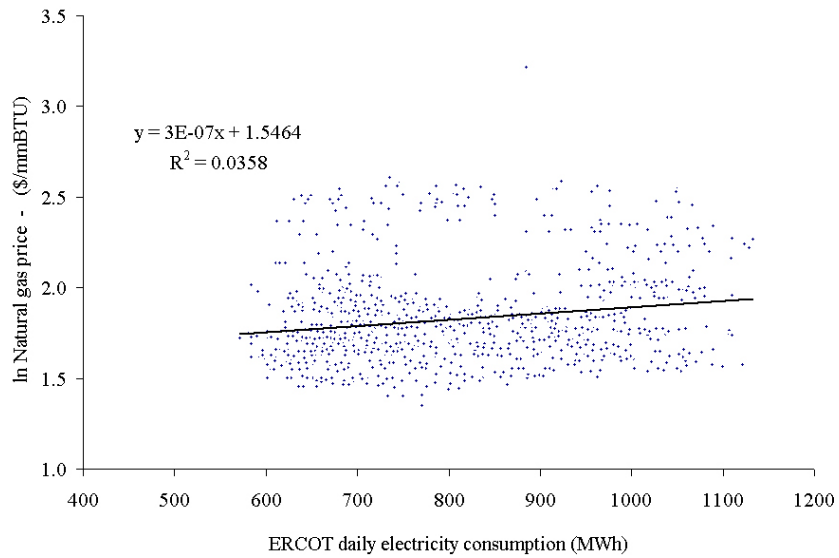


Figure 2.12: ERCOT daily electricity consumption vs. ln natural gas daily spot price from 2003 to 2005

separation point of two price regimes for the cash price. Before 2003, there was no consistent pattern of up or down. For example, the spike in late 2000 to early 2001 eventually came down to the price level before that. However, price spikes after 2003 were never followed by a price level lower than the previous low. That is, starting from 2003, the prices have been climbing along the support trend, with several noticeable price spikes, especially in early 2003 and late 2005. Based on this observation, we will study the correlation using 2003 as a separation time stamp.

An overview of the correlation between these two data series is shown in Figure 2.10. Overall the correlation is weak at about 23.2% or equivalently an R-Square of 5.4% ($23.2\% = \sqrt{5.4\%}$). When we separate the data before and after 2003 as shown in Figure 2.11 (1998-2002) and Figure 2.12 (2003-2005), we can see that such correlation is even weaker. Figure 2.11 shows an 18.93% correlation between these two data series from 1998 to 2002 and Figure 2.12 shows a 17.02% correlation after 2003.

Observation 2.3.A: Based on these observations of less than 30% correlations, we can conclude that generally speaking there is no relationship between these two data series [50].

2.3.3 Natural Gas Supply and Demand Factor

Usually there are two seasons for natural gas in term of natural gas storage utilization [2]. One is called injection season, which usually lasts from April to October. The rest of a year is called withdrawal season. The injection

or withdrawal of natural gas is determined by the supply and demand in the natural gas market. In injection season, the natural gas production outpaces the consumption and the surplus natural gas is injected into underground geological formation for later use in the withdrawal season when the consumption is larger than the production.

Since supply is usually larger than demand during injection season, we should expect a more stable price movement while the opposite for withdrawal season. Therefore, we study the correlation between HSC cash price and ERCOT electricity load in both seasons in this section. In our study, the injection season is defined as April 1st to October 31st and the rest of a year is the withdrawal season.

2.3.3.1 Injection Season

The results of this section are shown in Figure 2.13 through Figure 2.17.

Figure 2.13 shows an overview of the correlation for all the injection seasons from 1998 through 2005. It shows only about 18.7% correlation between these two data series during this period, indicating no relationship between them.

We then separate the data before and after 2003. Figure 2.14 shows the correlation before 2003. As we can see, the correlation is about 9.4% and there is no recognizable pattern. Figure 2.15 plots these two data series from 2003. Overall it still shows little correlation between them. Therefore, we are

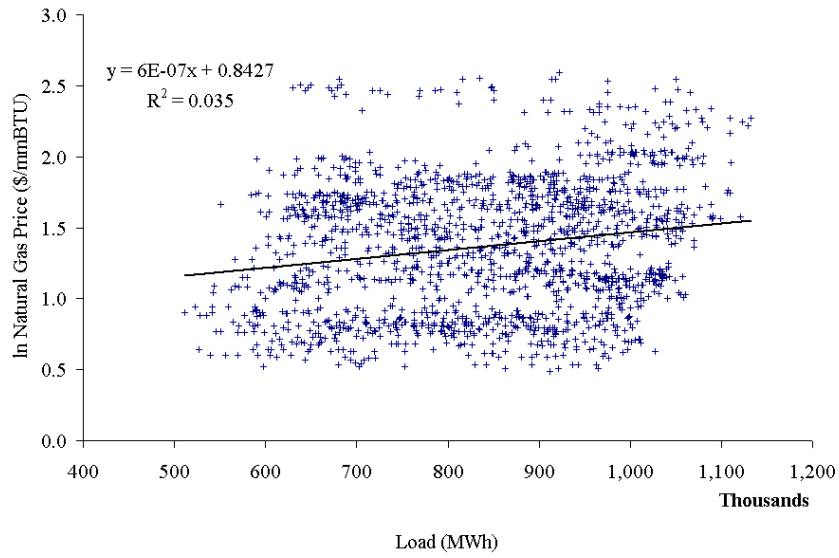


Figure 2.13: ln Natural gas spot price vs. ERCOT energy demand at injection season, 1998-2005

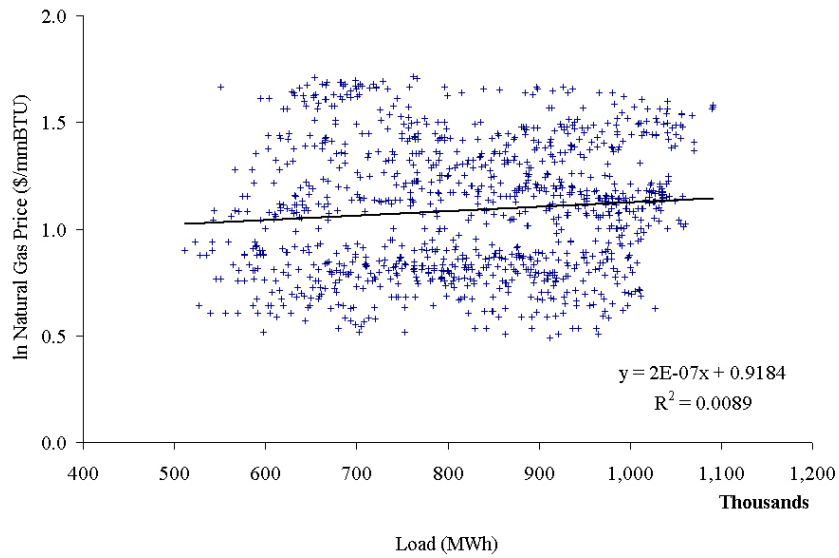


Figure 2.14: ln Natural gas spot price vs. ERCOT energy demand at injection season, 1998-2002

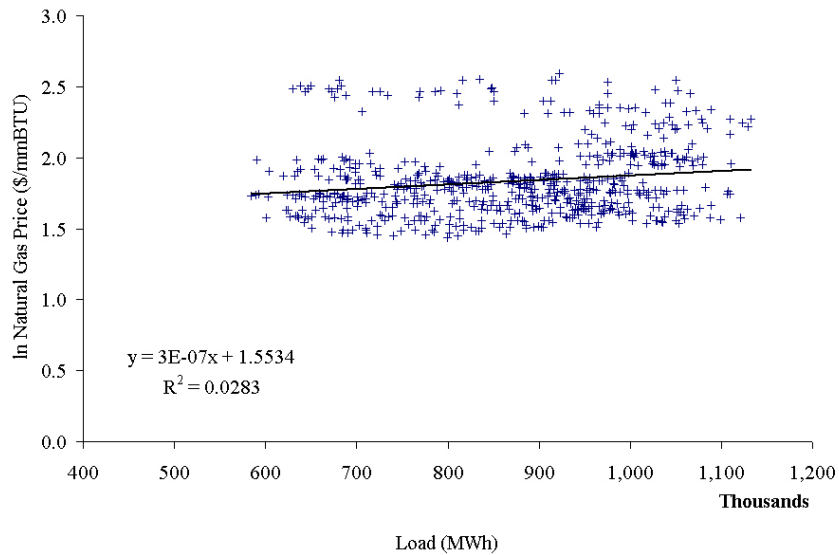


Figure 2.15: ln Natural gas spot price vs. ERCOT energy demand at injection season, 2003-2005

able to make the following observation:

Observation 2.3.B: There is no relationship between these two data series during injection season from 1998 to 2005.

2.3.3.2 Withdrawal Season

The results of this section are shown in Figure 2.16 through Figure 2.23.

Figure 2.16 shows an overview of the correlation for all the withdrawal seasons from 1998 through 2005. It shows 54.8% correlation between these two data series during this period. This is much higher correlation compared to the injection season, indicating that, due to the weather correlation between the

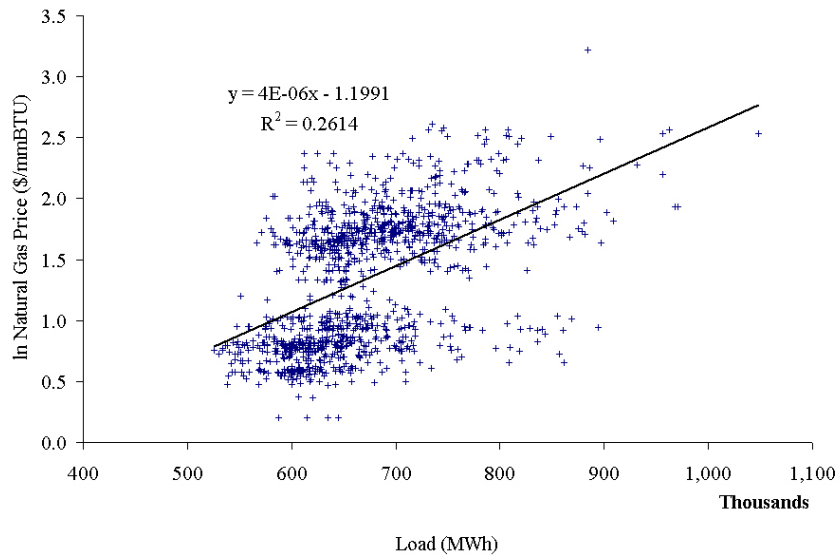


Figure 2.16: ln Natural gas spot price vs. ERCOT energy demand - withdrawal season

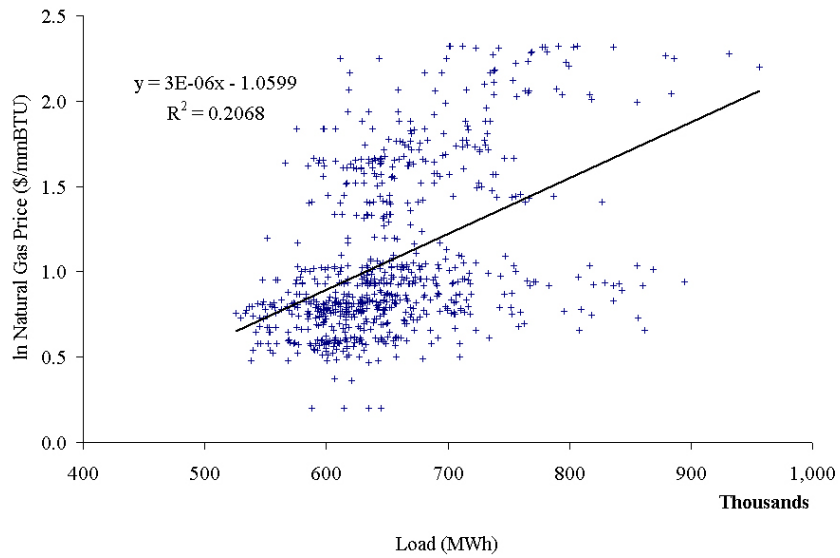


Figure 2.17: ln Natural gas spot price vs. ERCOT energy demand at withdrawal season, 1998-2002

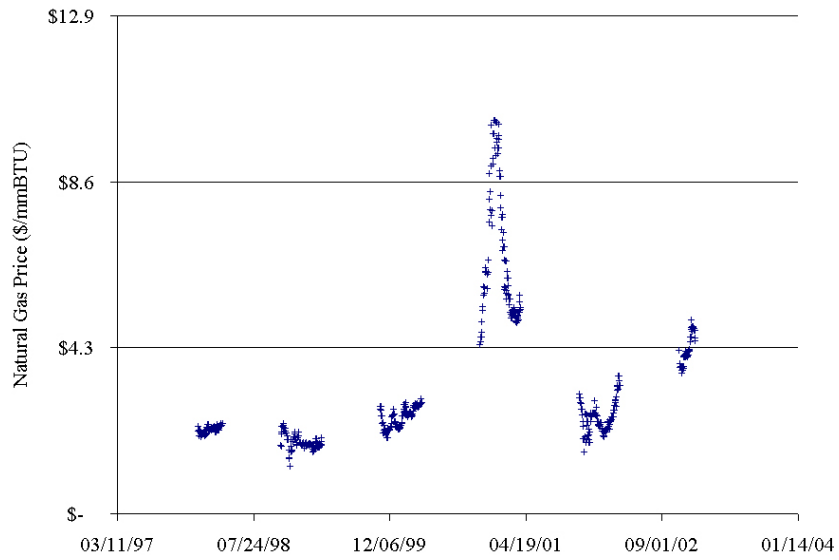


Figure 2.18: Time series of natural gas price during withdrawal seasons from 1998 to 2002

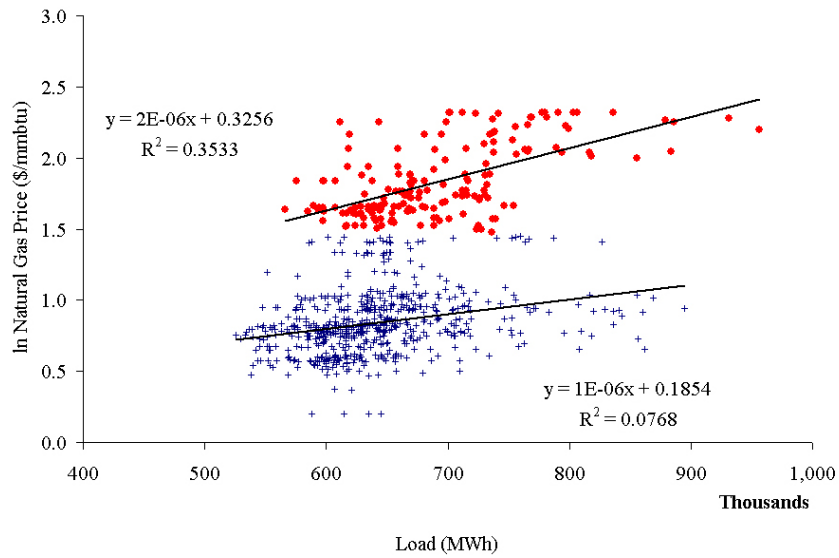


Figure 2.19: ln Natural gas spot price vs. ERCOT energy demand at withdrawal season, 1998-2002, threshold \$4.3

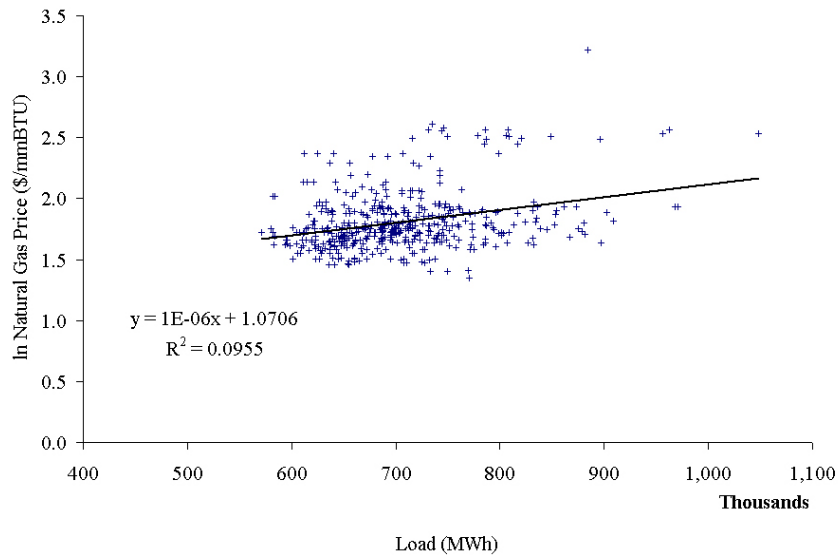


Figure 2.20: ln Natural gas spot price vs. ERCOT energy demand at withdrawal season, 2003-2005

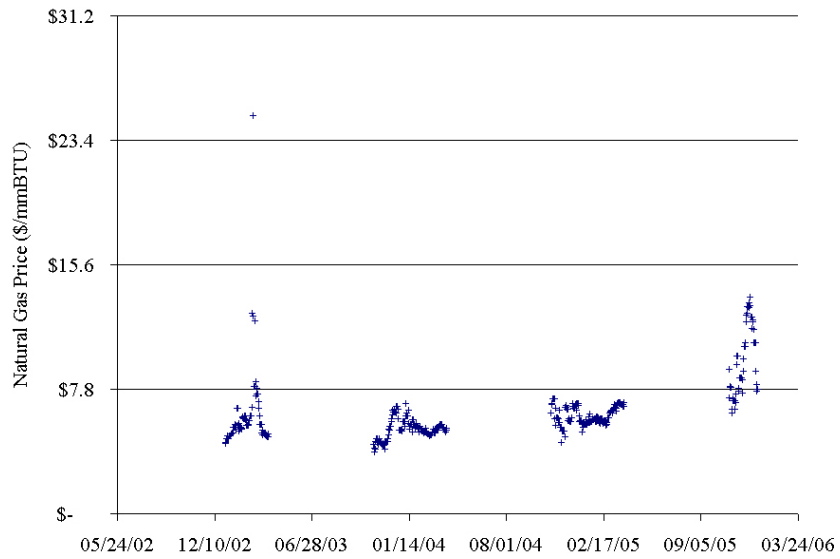


Figure 2.21: Time series of natural gas price during withdrawal seasons from 2003 to 2005

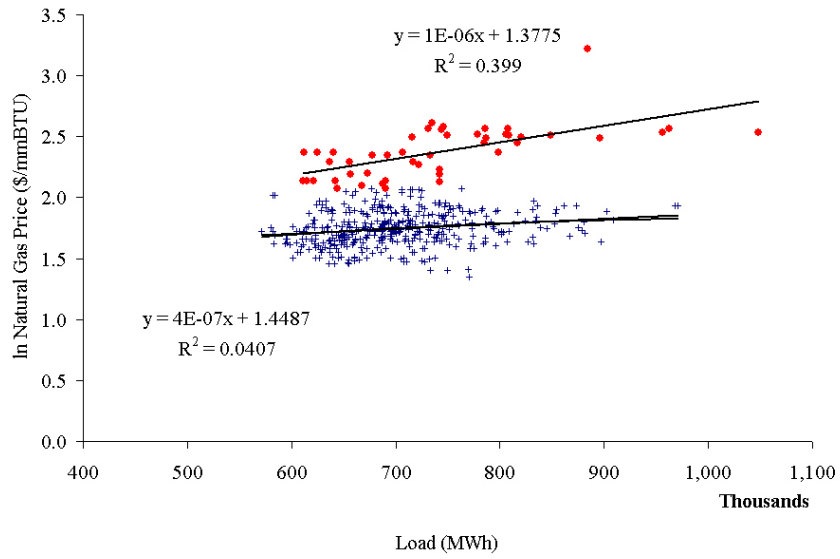


Figure 2.22: ln Natural gas spot price vs. ERCOT energy demand at withdrawal season, 2003-2005, threshold \$7.8

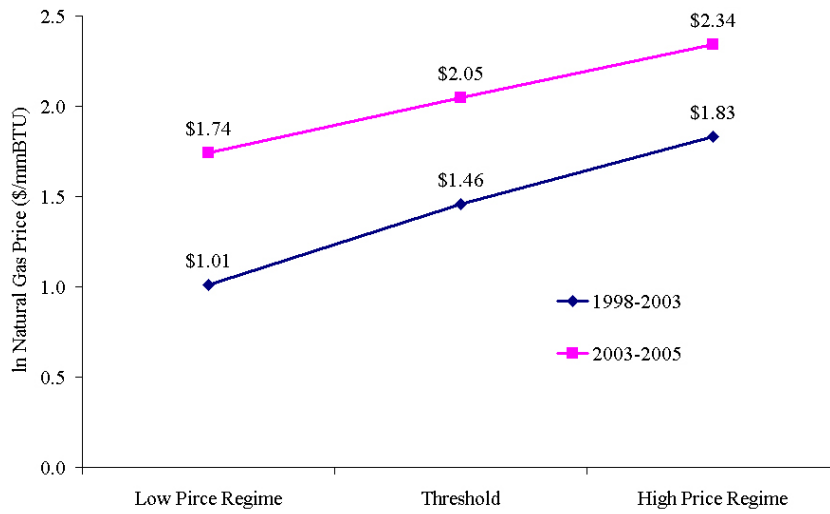


Figure 2.23: Average prices and threshold

ERCOT region and the whole US, the ERCOT electricity consumption plays a more important role in the supply/demand of HSC natural gas market.

As can be easily observed in Figure 2.16, there appears to be two price regimes with the low price regime centered at around \$2.10/mmBTU (equivalent ln price of 0.75) level and the high one at around \$5.75/mmBTU (equivalent ln price of 1.75) level. Our analysis shows that the low price regime mostly contains data from 1998 to 2002 and the high regime contains most data from 2003 to 2005, which is consistent with our previous finding in Section 2.2.

Figure 2.17 plots the HSC natural gas cash prices and ERCOT electricity load during withdrawal seasons from 1998 to 2002. We can see that the overall correlation between HSC natural gas cash price and ERCOT electricity load remains relatively low at 45.48%. Figure 2.18 shows the time series of HSC natural gas cash price during this period and Figure 2.19 plots the breakdown of these periods into two price regimes with a price threshold at \$4.3/mmBTU. We can see that when gas price is higher than \$4.3/mmBTU, as shown in Figure 2.18 during late 2000 to early 2001 and late 2002, it tends to stay at the above area for a period. During this period, the correlation between these two data series is much higher at 59.44% as shown in Figure 2.19, indicating a marked relationship. It also shows that when gas price is lower, there is barely any relationship between these two as the correlation is only 27.71%.

Analysis on the data from 2003 to 2005, as shown in Figure 2.20 to Figure 2.22, shows similar pattern. The overall correlation during this period is

30.90%, indicating weak relationship between these two data series. However, as the natural gas cash price spikes across the threshold of \$7.8/mmBTU, it tends to stay for a period of time. Also, during this time, the correlation between HSC natural gas cash price and ERCOT electricity load is 59.34%, which is almost the same as that during the period of 1998 to 2002. For other periods when HSC natural gas cash price is lower, there is no correlation between these two data series.

We also calculated that the average ln HSC natural gas cash prices at both price regimes and the price thresholds in both periods and they are shown in Figure 2.23. We then compared to the average ln price of low price regime, the threshold is about 0.35 higher and the average ln high price regime is about 0.71. In terms of actual price, they are 41.91% and 203.40% higher.

Based on these analyses, we have the following observations:

Observation 2.3.C: During withdrawal seasons, there exists a price threshold such that when HSC natural gas cash prices are higher than the threshold, there is approximately 60% correlation between these two data series. The value of the threshold has been higher as the overall level of the HSC natural gas cash price increases.

Observation 2.3.D: During withdrawal seasons, if we assume the low price regime represents the normal supply/demand in the HSC natural gas market, then when the HSC natural gas cash price goes up higher than 42%, we should expect a marked correlation (about 60%) between HSC natural gas

cash price and ERCOT electricity load and the average price during the HSC natural gas price spike is close to 100% higher.

2.3.4 Conclusions

In this section, we analyzed the relationship between HSC natural gas cash price, a major natural gas price index in ERCOT region, and ERCOT daily electricity load from 1998 to 2005. From the study, we can draw a general conclusion and a specific conclusion as follows.

2.3.4.1 General Conclusion

Although in general there is little correlation between these two data series, there are cases where a marked correlation exists, especially at the occurrences of major hurricane events and during withdrawal seasons, when the correlation can be as high as 60% indicating a fairly close relationship.

In an effort to model electricity prices using heat rate approaches, or evaluating heat rate options, one should take into account the potential correlations between natural gas spot price and electricity demand. The general assumption of the independence between the natural gas price and electricity holds during injection seasons with the exception of unpredictable events such as hurricanes. However, this assumption should be used with caution at withdrawal seasons, especially when a jump diffusion model is used in modeling the natural gas price.

Detailed study on the correlation between the natural gas price and the

electricity load at the interested ISO region needs be carried out before the non-correlated assumption is employed.

2.3.4.2 Specific Conclusion

Validating the assumption of independence between the natural gas price and electricity demand/prices used in the optimal natural gas purchase strategy in [23] is a big motivation for the analysis of this section and we can conclude that the assumption is valid. In the ERCOT application of [23], the natural gas spot price is assumed to follow a mean-reverting process, independent from the ERCOT electricity price, which is represented by a two regime marginal heat rate (MHR) model directly driven by electricity load. Therefore, we are in fact assuming there is no correlation between natural gas spot price and electricity load, which as has revealed, could be invalid.

Since the application periods (the primary example and two other months in the comparisons) are in summer and, more importantly, no jump process is simulated in the natural gas prices movement, we can conclude that we are able to use the assumption of no correlation between the natural gas price and electricity load is valid based on the general conclusion of this section.

Chapter 3

Short-Term Natural Gas Supply Optimization

Natural gas fired power plants (NGFPPs) are important electricity generation resources in the United States. Optimizing the natural gas supply portfolio, especially the short-term portfolio, is critical for the day-to-day operations and the financial performance of NGFPPs. Traditionally such optimization problems are solved using cost-minimization based frameworks. However, such frameworks are facing challenges due to the lack of consideration of associated financial risks in the current deregulated electricity markets, which are now born by the electric utility companies (EUCs) who own and operate NGFPPs.

In this section we present a utility-maximization based framework to optimize the short-term natural gas supply portfolio for the EUC. It considers the financial risks associated with the portfolio and incorporates the risk preferences of the EUCs as the decision-maker (DM) in the portfolio optimization process. An application of the proposed framework is provided and its results show that the proposed framework is more desirable in terms of risk-cost trade-off optimization.

3.1 Introduction

With the evolution of natural gas markets, electric utility companies (EUCs) can now purchase natural gas for natural gas fired power plants (NGFPPs) with great flexibility. For example, natural gas can now be purchased either through bilateral contracts, or through spot markets [60]. An EUC's natural gas portfolio consists of various natural gas contracts with different pricing and supplying conditions, and could be long-, mid-, or short-term in terms of time span. Among them, the short-term portfolio, with time frame ranges from one day to less than a year, is the most operation oriented as it has direct impacts on how EUCs operate NGFPPs.

Constructing an optimal natural gas portfolio, which is also known as the optimal supply mix problem, concerns the optimal purchasing, storage, transportation, and delivery of natural gas. This problem has historically been formulated based on expected cost-minimization frameworks with little concern for the associated financial risks, although most of the traditional frameworks address some other risks such as demand uncertainties [45], [7], [16], [21] and [44]. Such expected cost-minimization approaches are referred as *traditional approaches* in the rest of the section.

In a restructured electricity market, EUCs no longer enjoy regulated returns and are solely responsible for any financial risk and consequence associated with their natural gas portfolios. Traditional approaches do not systematically model the various associated risks, which has made them less suitable for the evolving markets. Furthermore, the embedded *risk neutral* assumption

in the expected cost-minimization framework could lead to riskier decisions [84] and [71]. An optimal short-term natural gas portfolio is desired that incorporates risk tolerance.

One theoretical framework based on modern portfolio theory for determining the optimal allocation between two types of different priced natural gas is first proposed in [35], but it does not take into account the detailed engineering and practical constraints, nor does it model the possible interactions with electricity markets. The lack of a theoretically sound and practical framework has resulted in many practitioners in the electricity industry relying on traditional frameworks or their experience from the regulated markets, while optimal risk-cost trade-off frameworks have been explored and applied to risk management in other sectors of deregulated electricity markets [42], [33], [63], and [73].

In this chapter, a utility-maximization based framework for constructing an optimal risk-cost trade-off short-term natural gas portfolio for NGFPPs is proposed to meet these upcoming challenges in the emerging competitive power and natural gas markets. The proposed framework improves on traditional approaches not only by systematically modeling various risk factors and the risk preferences of EUCs, but also by modeling the interactions between EUCs and two related markets: the natural gas spot markets and the electricity spot markets, features which are not present in the previous literature. As will be shown later in the application, the proposed framework has a clear advantage in achieving an optimal risk-cost trade-off.

The remainder of the chapter is organized as follows. Section 3.2 presents the characterization and details of the risks involved and Section 3.3 presents the proposed cost-risk framework. Section 3.4 shows the modeling approach. An application is shown in section 3.5 to illustrate the procedure and benefits of using the proposed framework and section 3.6 concludes the section.

3.2 Risk Characterization

In this section, we discuss the volatility behaviors in both natural gas prices and demand.

3.2.1 Volatility in natural gas spot markets

The deregulation of the natural gas markets has not only had direct impacts on the spot prices, but has also brought uncertainties, especially in recent years when the annualized volatility for natural gas price has been over 60% and increasing [54]. Figure 3.1 shows the time series of the daily settled spot price of natural gas in Henry Hub since January 2000.¹

As will be shown later, the volatility of natural gas spot prices has impacts on the selection of the optimal portfolio. Therefore, it is important for EUCs to have correct market outlooks. Market outlooks, which include the management's expectation for market index prices and volatilities fore-

¹This percentage has been lowered as TXU announced the constructions of several new coal fired power plants.



Figure 3.1: Natural gas spot price of Henry Hub since 2000

casts, are critical in using the proposed framework as these are the fundamental assumptions. The process requires in-depth knowledge of current market conditions and both fundamental analysis such as economic growth, monthly weather outlook, natural gas storage levels, etc, and technical analysis including studies of historical price paths. Interested readers can refer to [85] for more details.

3.2.2 Volatility in natural gas demands

Because of the excellent peaking ability of NGFPP, EUCs usually use them to follow electricity loads.² NGFPP have become a significant source of peaking generation. During the last five years, 98% of power plants built were NGFPP. Furthermore, 95% of announced power capacity addition through 2010 is gas fired [67].³

²It is worth pointing out that some types of NGFPP, such as natural gas combined cycle (NGCC) systems, are usually used as base load units.

³This percentage has been lower since TXU announced its plan for new coal fired plants.

Short-term electricity demands are affected by various factors and could be very sensitive to some factors such as weather [26], [24]. Uncertainties in electricity demands would have immediate impacts on natural gas consumption of NGFPP and cause significant volatilities as it would affect the optimal unit commitment. Therefore, it is important to take this issue into consideration.

In the proposed framework, addressing this aspect requires the integration of accurate short-term load forecasting (STLF) and an optimal unit dispatch/commitment algorithm, which distinguishes the proposed framework from traditional approaches in the following two aspects.

Firstly, STLF is conducted and an optimal unit dispatch/commitment problem is solved to produce expected daily consumptions. Solving the optimal unit dispatch problem requires certain assumptions about the electricity market such as electricity prices and operation status of the power plants of EUCs. Discussion of the unit dispatch/commitment problem is beyond the scope of this chapter and interested readers can refer to [8], [87]. This integration is able to provide much more details than that of traditional approaches.

Secondly, daily demand variations are introduced through Monte Carlo simulations, representing the stochastic nature of the natural gas consumption. As will be shown later, due to the interaction between NGFPP consumption and various markets, as well as the complex structures of various natural gas products, it is infeasible to solve the problem analytically. Therefore, we adopted Monte Carlo simulation as an effective way in modeling and optimization. Although such implementation significantly increases the optimization

workload, it is able to simulate the actual demand fluctuations in a much more accurate and realistic way.

3.3 Risk-Cost Framework

The proposed risk-cost framework is based on classic return-risk utility theory framework, which models the risk preferences of the decision-maker (DM) by measuring the trade-off between risks and expected return.

During the decision making process of optimal natural gas portfolio selection, the DM could choose among feasible portfolios with different expected profits, i.e. revenue-cost, denoted as r , and associated risks, denoted as σ . For a particular risk level, there is one or more portfolios that would achieve the highest expected profit. These portfolios then form the efficient-frontier along the feasible risk levels as shown by the solid concave curve in Figure 3.2. On the other hand, DM is indifferent for portfolios that bring the same utility level for them, which can be represented by an iso-utility curve as shown by the convex dotted curve in Figure 3.2. The optimal portfolio theory suggests that optimal choice is the one that is the tangent point between the iso-utility curve and the efficient frontier, which is shown as the black square dot in Figure 3.2.

The utility of DM is a function of profit r and risk σ , i.e.

$$U = U(r, \sigma) \tag{3.1}$$

where $r = p - c$ and p is the price and c is the cost.

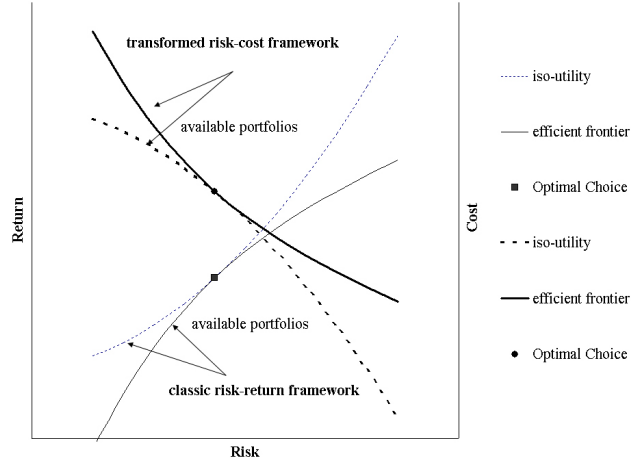


Figure 3.2: Classic risk-return framework and the proposed risk-cost framework and their efficient frontiers and the iso-utility curves

Substituting r in (3.1), we have:

$$U = U(p - c, \sigma) \quad (3.2)$$

In the electricity industry, electricity is usually sold at retail at pre-determined prices, i.e. p has been fixed.⁴ Therefore, (3.2) has become:

$$\tilde{U} = \tilde{U}(c, \sigma) \quad (3.3)$$

The classic risk-return framework is now transformed into the proposed risk-cost framework. The graphic representation is also shown in Figure 3.2, where the originally convex iso-utility (concave efficient frontier) curve becomes concave (convex) instead.

⁴We do not consider the scenario where generation capacity surplus or shortage causes retail price to fluctuate significantly.

3.4 Modeling Approach

This section first presents the interactions among natural gas consumption with various markets, followed by brief discussions on modeling risk preferences of EUCs and the integrated simulation-optimization algorithm used in the proposed framework.

3.4.1 Interaction with Markets

The natural gas consumption of NGFPP is not stand alone or only related to the natural gas portfolio. In fact, it is closely related to various markets. Figure 3.3 is a graphical presentation of the relationship among the natural gas consumption of NGFPPs and the natural gas portfolio, as well as other markets such as natural gas and electricity markets.

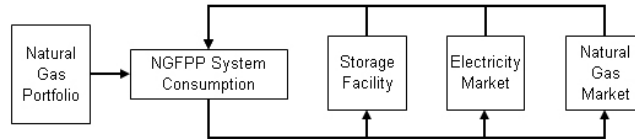


Figure 3.3: Interaction with markets

The wholesale electricity market serves as an important part in the decision making process. In a deregulated electricity market, EUCs are able to purchase electricity from bilateral and/or the spot electricity markets to meet demands. For example, when market implied marginal heat rate, or MHR, which is the equivalent heat-rate calculated using the clearing price for energy divided by the prevailing natural gas price, is lower than the marginal production heat rate of EUCs, EUCs might want to purchase power instead of

generating themselves. This is related to the so-called spark spread and [95] provides more detailed discussion.

As illustrated in Section 3.2, electricity market assumptions are required in producing short-term natural gas demand forecasts. Therefore, modeling electricity markets requires consistent electricity market outlooks as an embedded assumption.

These interactions bring more complexities in selecting the optimal natural gas portfolio by introducing more options and they need to be modeled specifically to reflect the characteristics of each market.

3.4.2 Natural Gas Products in Current Markets

Three major types of natural gas products in current natural gas markets are considered in the model. They are described and modeled as follows.

Base load gas (BLG)

BLG contracts provide natural gas to the EUCs at a 24/7 non-stop fixed flow rate throughout the contracted period. The flow rate x^{BLG} , a decision variable, is determined through negotiation. Its price P^{BLG} , a parameter, is usually settled at the monthly price index. The daily cost for BLG is:

$$24 \times x^{BLG} \times P^{BLG} \tag{3.4}$$

Intra-day gas (IDG)

IDG contracts also provide natural gas to the EUCs at a fixed flow rate x^{IDG} , a negotiated variable, throughout the contracted period. However, IDG

only flows at a certain negotiated time-window during a day. For example, an IDG contract can be set to deliver natural gas during on-peak hour from 7:00 to 22:00. The amount of IDG delivered at hour j is

$$x_{i,j}^{IDG} = \begin{cases} 0 & j \notin H^S, \dots, H^{S+T} \\ x^{IDG} & j \in H^S, \dots, H^{S+T} \end{cases} \quad (3.5)$$

where

i : day, $i \in 1, \dots, 30$,

j : hour, $j \in 1, \dots, 24$,

H^S : negotiated starting hour of IDG contract,

T : the length of natural gas delivery for IDG contract.

In actual practice, there is a minimum length requirement for IDG contracts, usually a 4-hour delivery time-window.

$$T \geq T^{MIN} \quad (3.6)$$

where T^{MIN} : minimum natural flowing period for IDG contract;

IDG is also a fixed priced natural gas product. Since its structure provides more flexibility for the EUCs, IDG is usually priced at a premium over settled monthly price index. The daily cost for IDG is:

$$T \times x^{IDG} \times P^{IDG} \quad (3.7)$$

where P^{IDG} : the price of intra-day natural gas (\$ /mmBTU).

Swing gas(SWG)

SWG is the most flexible product as its flow rate is on demand, i.e. it can swing to follow the consumption at anytime. It is also called floating priced gas as it is usually priced at a premium over spot gas price, which means the daily cost for SWG is:

$$\sum_{j=1}^{24} x_{i,j}^{SWG} \times P_i^{SWG} \quad (3.8)$$

where

x^{SWG} : the flow rate of swing gas,

P^{SWG} : the price of swing gas (\$ /mmBTU).

3.4.3 Storage Gas (SG)

Besides these three major types of products, there is another type of natural gas product that is usually not available on the market. That is, the natural gas from the storage facility (SG).

A storage facility usually is a geologic structure such as a depleted underground natural gas reservoir or an artificial structure such as pipelines, which are able to pack the gas at the time of low demand. Although there are fees associated with activities using the storage facility such as injection and withdrawal and other limits, storage facilities have provide tremendous value to EUCs [53] [91]. When storage facilities are not able to accommodate the excess gas, the EUC would have to sell the excess gas back to the spot markets.

For SG, there are physical limitations for withdrawing and injecting natural gas into SG at any hour. Also there usually is a limit on the aggregated NG surplus/deficit on the storage facility:

$$-C^{SFW} \leq \sum_{i,j} x_{i,j}^{SFI} - \sum_{i,j} x_{i,j}^{SFW} \leq C^{SFI} \quad (3.9)$$

where

C^{SFW} : the max amount of natural gas deficit allowed from storage facility at the end of month,

x^{SFI} : the flow rate of natural gas injected to the storage,

x^{SFW} : the flow rate of natural gas withdrawn from the storage,

C^{SFI} : the max amount of surplus natural gas remained in the storage facility at the end of period.

The daily cost of using SG is:

$$\left\{ \sum_{j=1}^{24} x_{i,j}^{SFI} + \sum_{j=1}^{24} x_{i,j}^{SFW} \right\} \times P^{SG} \quad (3.10)$$

where P^{SG} : cost for natural gas transactions (injection/withdrawal) in the storage facility (cent/mmBTU);

3.4.4 Daily cost of natural gas

Since NGFPP must meet its electricity demand at any time, it needs to either supply enough natural gas for generation or buy electricity from the

spot markets. That is, natural gas supply and consumption must be balanced at any time:

$$\begin{aligned} x^{BLG} + x_{i,j}^{IDG} + x_{i,j}^{SWG} + x_{i,j}^{SFW} + x_{i,j}^{ElectricityPurchase} \\ = L_{i,j} + x_{i,j}^{SFI}, \forall i, j \end{aligned} \quad (3.11)$$

Equation (3.11) indicates that at any day i and hour j , the natural gas consumption must be equal to the sum of the four types of natural gas resource (BLG , IDG , SWG and SG) together with the electricity purchase (translated to the equivalent amount of natural gas required for generation). SG is used for injection ($x_{i,j}^{SFI}$) when BLG and IDG exceeds the demand $L_{i,j}$. In this chapter, we exclude the scenario where excess natural gas could be sold to the spot markets.

3.4.5 Risk preferences of EUCs

The risk preference of the EUC are the key issue as it reflects the management's attitude towards risk-cost trade off and is the core of the framework. For example, a very conservative EUC management may choose to avoid risk exposures whenever possible and prefer fixed priced natural gas even if the floating priced natural gas had a significantly lower expected price.

The empirical DM utility function possesses the following quadratic form [35]:

$$\tilde{U} = A\sigma^2 + b\sigma - c \quad (3.12)$$

where \tilde{U} is the utility, σ and c are the financial risk and the expected

cost of the portfolio, respectively. Parameters A and B are estimated through a survey. A negative coefficient A indicates that the DM is risk averse, i.e. the DM achieves his/her maximum utility for a given cost at a certain risk level. It reflects the degree of risk aversion, i.e. more negative A indicates a more conservative DM. These two parameters could vary as the management style varies.

Estimation of risk preferences of EUCs could be assessed by conducting surveys on the management team. Interested readers can refer to [100] for more details.

3.4.6 Objective function

The daily cost (DC_i) of natural gas is the sum of cost for all natural gas products:

$$DC_i = 24x^{BLG}P^{BLG} + x^{IDG}TP^{IDG} + \sum_{j=1}^{24} x_{i,j}^{SWG}P_i^{SWG} + (\sum_{j=1}^{24} x_{i,j}^{SFI} + \sum_{j=1}^{24} x_{i,j}^{SFW})P^{SG} \quad (3.13)$$

The objective of the proposed framework is to maximize the expected utility of EUCs:

$$\max \tilde{U} = A\tilde{\sigma}^2 + B\tilde{\sigma} - C \quad (3.14)$$

where:

$$C = EXP(\sum DC_i),$$

$$\tilde{\sigma}^2 = VAR(\sum DC_i).$$

3.4.7 Integrated simulation-optimization algorithm

The underlying optimization problem is essentially a mixed integer non-linear programming, or *MINLP*, problem. In actual practice, there are certain restrictions on the natural gas productions. Besides the minimum time window requirement for IDG as mentioned in Section 3.4-B-2), the incremental volumes of natural gas for all these types are multiples of a certain step. For example, orders of a certain type of gas may need to be in multiples of 5,000 mmBTU/Day, i.e. no order of 62,700 mmBTU/Day will be accepted: the volume nomination needs to be either 65,000 or 60,000 mmBTU/Day. Thanks to this fact, we are able to enumerate all possible solutions and then solve this problem using an integrated simulation-optimization algorithm.

Monte Carlo simulation is utilized to generate scenarios of natural gas prices, market implied MHR, and natural gas consumption of NGFPP. These are generated using simulation of their estimated parameters, together with the forecasted market outlooks that were discussed in Section II. Optimization is then performed to find optimal solution by testing all possible solutions under generated scenarios. Such integrated simulation-optimization algorithms could also be found in financial optimization applications [102], [66].

3.5 Applications

This section demonstrates the proposed framework by an application in selecting optimal portfolio for an EUC in the ERCOT region whose loads are mostly residential load with peak demand at around 3,000 MW and service

population of about one million people. The EUC owns and operates several NGFPP and uses them to follow the electricity consumption.

In this section, the model setup is presented first, followed by the results and discussions of advantages of the proposed framework over other methods, and then some caveats.

3.5.1 Model setup

Natural gas products

All the four types of natural gas products (*BLG*, *IDG*, *SWG* and *SG*) are included in the portfolio. The price of BLG (P^{BLG}) is set to be \$ 6.0/mmBTU and the price of IDG (P^{IDG}) is set at \$ 6.1/mmBTU. The incremental volume for BLG is 5,000 mmBTU/Day and 2,000 mmBTU/day for IDG. The SWG (P^{SWG}) is set to have an expected price of \$ 5.5/mmBTU with monthly volatility at \$ 0.75/mmBTU. The operation cost of SG is set to be \$ 0.12/mmBTU for both withdrawal and injection.

The interaction with the electricity market affects the amount of natural gas withdrawn or injected to the SG. The hourly flow rate of natural gas withdrawn is:

$$x_{i,j}^{SFW} = \min(F^{SFW}, L_{i,j} - x_{i,j}^{BLG} - x_{i,j}^{IDG}) \times \omega, \forall i, j \quad (3.15)$$

where

F^{SFW} : max flow rate of natural gas withdraw from the storage facility;

ω : 0 when the market implied MHR is higher than the own marginal production heat rate, and is 1 otherwise.

$L_{i,j}$: forecast natural gas consumption at hour j in day i , a stochastic variable;

The hourly flow rate of natural gas injection is:

$$x_{i,j}^{SFI} = \min(F^{SFI}, x_{i,j}^{BLG} + x_{i,j}^{IDG} - L_{i,j}) \times \xi, \forall i, j \quad (3.16)$$

Where

F^{SFI} : max flow rate of injecting natural gas into the storage facility;

ξ is 0 when the market implied MHR is lower than the own production MHR, 1 otherwise.

Natural gas spot market

EUCs can sell the excess natural gas back to market if SG is not able to store them. However, we limit the amount of sale to excess amount only, i.e. EUCs are not allowed to sell more than excess gas even if the market spot price is higher than the cost of SG. This is simply due to the corporate policy and it could be different for other EUCs.

We use the mean-reverting process in modeling the spot gas price and the parameters are estimated using available historical prices. More details and techniques on modeling natural gas market, such as mean-reverting process, and estimating related parameters can be found in [14], [15], and [48].

Electricity market

The interaction between NGFPP and electricity markets, i.e. whether to use SG or not, is triggered by the electricity market's implied MHR. When implied MHR is higher than the marginal production heat rate, NGFPP is better off by generating electricity itself, otherwise purchasing from the electricity market is preferred. However, the NGFPP is modeled such that it is not selling its excess capacity even when the market condition is favorable for doing so.

Figure 3.4 shows relationship between the actual load of the EUC studied in our application and the actual ERCOT market implied MHR from June 2004 to August 2004. There are apparently two MHR regimes. One of them, the lower MHR areas, which we refer to as the *normal regime*, shows a strong correlation between market implied MHR and the loads of EUC, while the other, much higher MHR area, which we refer to as the *abnormal regime*, shows the randomness of high MHR over a certain range of load.

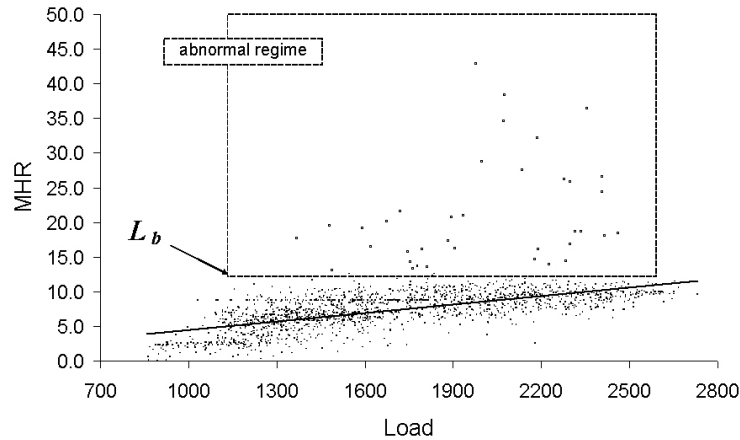


Figure 3.4: Two-regimes jump diffusion model of balancing energy prices

Based on these available historical load and implied MHR data, we adopt a similar two-regime structural price model to that in [10], [59] but use the two regime model to represent MHR in ERCOT, instead of modeling electricity prices as in many other approaches. In particular, based on regression of data from the normal regime and a uniform probability distribution model of price in the abnormal regime, we model the MHR as:

$$MHR_t = \begin{cases} 4.075 \times 10^{-3} \times L_t + 0.439 + 1.817 \times \epsilon_{st} \\ \text{if}(L_t \leq 1,183) \text{ or } \kappa_t = 0 \text{ [normal regime]} \\ \\ \nu(13, 50) \\ \text{if}(L_t \geq 1,183) \text{ or } \kappa_t = 1 \text{ [abnormal regime]} \end{cases} \quad (3.17)$$

where

MHR_t : the implied MHR in the balancing electricity market,

L_t : the demand at time t for the EUC,

ϵ_{st} : a standard normally distributed random variable,

$V(13, 50)$: the uniform distribution between 13 and 50;

1,183 MW: the break point of high heat rate regime and low heat regime,

κ : an independent random variable with the following distribution:

$$\begin{cases} p(\kappa = 1) = 4.61\% \\ p(\kappa = 0) = 95.39\% \end{cases} \quad (3.18)$$

3.5.2 Modeling risk preferences

A survey of the management team of the EUC has been conducted [35] to determine the DM utility function. The empirical DM utility function possesses the following quadratic form:

$$\tilde{U} = -8.0178 \times 10^{-5} \times \sigma^2 - 3.7688 \times 10^{-3} \times \sigma - c \quad (3.19)$$

where σ is the volatility and c is the cost of the interested project or portfolio.

3.5.3 Results and discussions

In this section, first we illustrate the obtained optimal natural gas portfolio structure using a daily snapshot. Then a sensitivity analysis for different natural gas market outlooks is presented. Finally, we compare the optimal results with those derived using two other methods.

Optimal portfolio structure

Figure 3.5 illustrates the solved optimal portfolio structure and the corresponding natural gas consumption profile of a typical day. Although we only show one day's profile here, readers should keep in mind that the optimal portfolio structure is solved using the probability distribution of the daily consumption profile over a month instead of picking the profile of a typical day or average day. The differences of using these alternatives will be discussed in the next section.

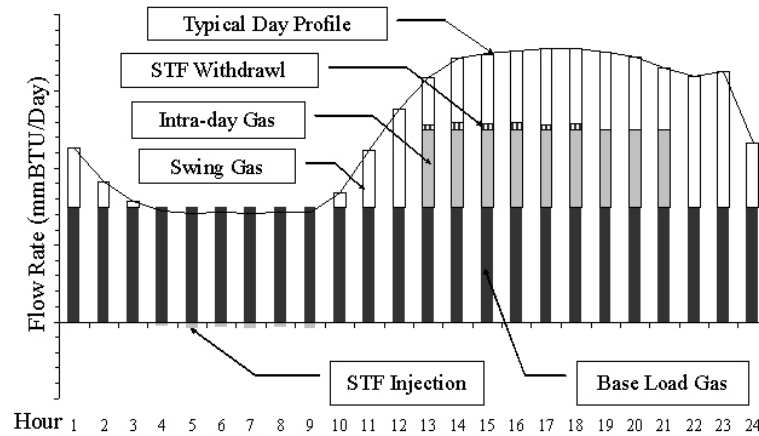


Figure 3.5: Optimal natural gas portfolio

As indicated in Figure 3.5, BLG is the component which forms the base of the portfolio. It provides natural gas at a fixed flow rate over 24 hour period and is shown as the black bars. IDG is at the center grey bars ranging from Hour 13 to Hour 21. The rest of the natural gas consumption need is filled by SWG. SG is utilized to cycle the natural gas. For the typical profile shown in Figure 3.5, SG is used to inject excess natural gas from Hour 4 to Hour 9 when BLG exceeds the consumption needs and the injected gas is withdrawn later in the day to meet demand. SG helps reducing the volatility of the portfolio by acting as SWG without paying the spot price. In Figure 3.5, the interaction with real-time energy market is not shown, but should that purchase happen, some portion of the swing gas will not be needed.

Impacts of market outlooks

As pointed out in Section 3.2, one important assumption when utilizing

the proposed framework is the market outlook and volatility estimations by the EUC. The assumption will affect the intrinsic risk level of the optimal natural gas portfolio, which reflects on the SWG percentage (floating priced): the higher the SWG percentage, the more exposure to the natural gas spot market price risks.

Figure 3.6 shows the impacts of different market outlooks to the EUC in our example. It plots the SWG percentage of the optimal natural gas portfolio at different natural gas spot market price volatility outlooks. It shows clearly that the SWG ratio decreases as the expected volatility increases. In this particular setup, for example, the percentage of SWG is 35% when the expected natural gas spot market price volatility is 65 cents. However, the percentage decreases to 25% when the price volatility estimation increases by only 10 cents to 75 cents. The decrease is due to the risk averseness of the EUC in this case, i.e. the EUC will try to reduce the exposure (SWG percentage drops 10%) to the market price volatilities if the market is expected to be more volatile (volatility increases by 10 cents).

The impact of market outlooks depends on the degree of risk averseness of the EUC. It could be dramatic as shown in Figure 3.6. Therefore, caution needs to be exercised when developing market outlooks.

Comparisons

The output from the proposed framework is compared to the result obtained using average daily profile, referred to as the *average profile*. In

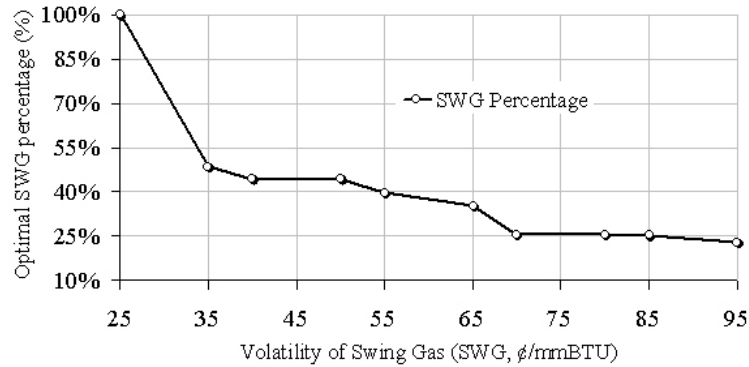


Figure 3.6: Optimal floating ratio at various volatilities

contrast to the proposed method, using the average daily consumption profile does not consider the fluctuation of daily natural gas consumption. Such approach reduces the computation burden and it is much easier to understand and implement.

The output from the proposed framework is also compared with the result from an experienced trader who developed a portfolio independently, referred to as the *Trader's strategy*. The trader makes the decision of buying different natural gas types based on his own experiences and expectations including his market outlooks, operational constraints, etc. This benchmark is introduced since this is the typical practice in the current electricity industry due to the lack of aids from appropriate practical models.

The graphical presentations of the comparisons of three methods for three different months using the risk-cost framework presented in Section 3.2 are shown in Figure 3.7 and detailed comparisons of risk and cost per mmBTU

for the three methods are shown in Table 3.1.

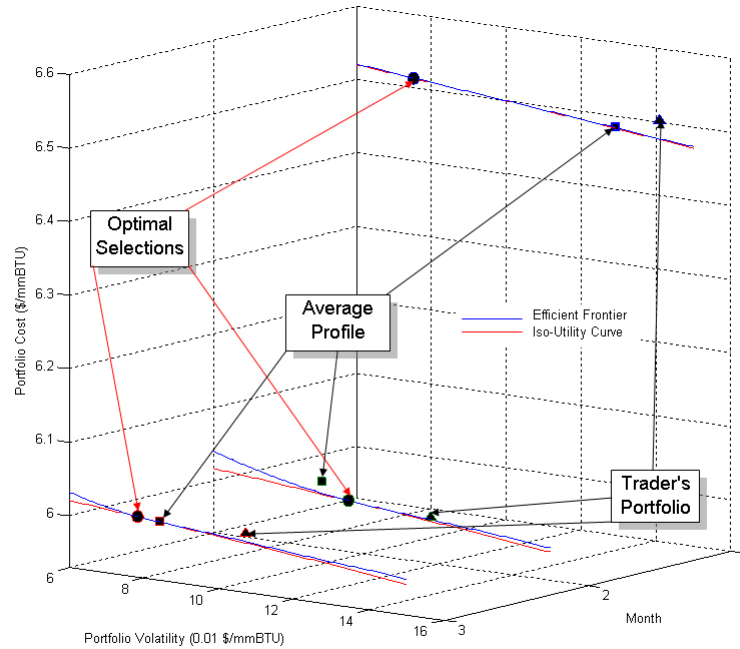


Figure 3.7: Comparison of outputs of the proposed framework for three months

	Month	Proposed Framework	Average Profile	Trader's Portfolio
Risk (€)	1	7.50	12.90	14.10
Cost (\$)		6.51	6.49	6.50
Risk (€)	2	9.60	8.90	11.80
Cost (\$)		6.00	6.02	5.99
Risk (€)	3	7.80	8.40	10.70
Cost (\$)		6.01	6.01	6.01

Table 3.1: Comparisons of results from three methods

It could be seen clearly from Figure 3.7 and Table 3.1 that neither the result obtained by using average profile or the trader's strategy are on the efficient frontier, which indicates that neither is optimal at the given risk levels. For example, both methods are riskier than the output from the proposed

framework in Months 1 and 3 as shown in Table 3.1. In Month 2 the method of using average profile is more conservative, while the trader's portfolio is riskier. The comparisons also show a great feature of the proposed framework in that it could serve as a benchmark to evaluate the trader's performance in constructing the natural gas portfolio, as well as evaluating the trader's risk preference. In this case, it is shown that the trader consistently tends to take more risks.

3.6 Conclusions

A utility-maximization based framework to select the optimal short-term natural gas supply portfolio for EUCs who own and operate NGFPPs is proposed in the section. It aids the decision making by systematically modeling the risk preferences of EUCs and the stochastic nature of various key variables. It is more desirable than traditional cost-minimization based frameworks because it is able to provide an optimal risk-cost trade off, which is lacking in the traditional framework, and it also systematically models key risk factors through detailed simulations, which is more realistic. Its application in an EUC is presented and the results have clearly shown the improvements over other methods. This framework can also be extended to evaluate mid- to long-term optimal strategy by simply expanding the study time frame. Future research includes study on how changes in the risk preferences of EUC management affect the optimal results and how to integrate this framework into enterprise-wide risk management, etc.

Chapter 4

Determining Optimal Structure for Insurance on Generation Forced Outage

Insurance on generation forced outages (IGFO) is usually actuarially priced under a certainty equivalent framework instead of using complete market pricing theory. The feasibility structure index (FSI) of an IGFO is defined as the spread between the upper bound of the purchase price that the insurance buyer (the electric utility company) is willing to pay and the minimum selling price that the insurance seller (the insurance company) is willing to sell. It is an indicator of whether negotiating a certain IGFO structure makes business sense or not. FSI is not only a function of certain objective factors such as expected market prices and volatilities, but also of certain subjective variables, including each party's risk tolerance level and bilaterally negotiated deductibles.

In this chapter we study the relation between FSI and these key subjective factors. We also show that higher probability of price spikes and aggregated insurance could effectively narrow the FSI.

4.1 Introduction

Generation forced outage, or GFO, generally refers to unplanned generation outages that causes generation units to be de-rated or out of service. Such events usually cannot be fully predicted or prevented without reliability centered maintenance such as that of the airline industry, which is uneconomic for the EUCs in term of costs and benefits.

Before electricity market deregulation, there was not much incentive for the electricity utility companies (EUCs) to hedge the financial consequences associated with GFO. When GFO occurred, the associated financial loss could eventually be recovered by ex post adjustment of tariffs charged to customers. However, in a competitive power market, EUCs have to bear all the associated financial loss, which could be tremendous. For example, for a generation unit with an average output of 200 MW and an average production cost of \$50/MWh, when it is forced out of service for 2 weeks and the average spot market price for electricity is \$80/MWh during the GFO period, the total replacement cost of energy will be \$5.38 millions and the financial loss will be \$2.02 millions.

Because of such possible adverse financial consequences, new financial tools have been developed to hedge against financial losses associated with generation forced outages. One such innovative product is the insurance for generation forced outages, or IGFO. Reference [93] proposes a general structure of IGFO and used a Markov process model for electricity prices. Reference [47] discusses the importance of GFO protection with insurance as well as the

benefits with several real case studies. In real world business practices, IGFO is viable and some major providers like ACE America are active in the North America electricity markets [55].

An IGFO contract usually is a bilateral insurance contract between the insured (usually an EUC) and the insurer (usually an insurance company). Compared to other traditional hedging products such as vanilla electricity call options, IGFO has a cost advantage. This is because for call options, price is the only triggering factor. But a payout of an IGFO contract, as will be shown later, is triggered by two factors: 1) price and 2) GFO capacity. Such a double-trigger feature means that the IGFO claims are a subset of the claims for electricity call options having a comparable strike price, which not only reduces the cost of IGFO, but still is able to protect EUCs from the most adverse scenarios, i.e. GFO occurs when the replacement energy is expensive.

A utility maximization based general evaluation framework for IGFO is presented in [58]. In this chapter, we mainly focus on the feasibility structure index, or FSI, of IGFO, which is the spread between the maximum purchase price that the insured is willing to pay and the minimum selling price that the insurer is willing to sell. As will be shown later, quantifying FSI can help facilitate EUCs in the decision process by identifying the feasibility of a certain IGFO contract, better counter parties, and better strategies. We also show several factors that affect FSI. In the rest of the chapter, the terms *insured*, *insurance buyer* and *EUC* will be used interchangeably, as well as *insurer*, *insurance seller* and *insurance company*.

The remainder of this chapter is organized as follows: Section 4.2 briefly reviews the general structure of IGFO and the utility maximization based evaluation framework. Section 4.3 defines FSI and presents related formulas. Section 4.4 illustrates the concepts and calculations of FSI through a simplified example. Section 4.5 analyzes various factors that may affect FSI and Section 4.6 concludes this chapter.

4.2 Evaluation of IGFO Contracts

First we show the general structure of IGFO contracts.

An IGFO contract usually is a bilateral contract. Typically, at the commencement of an IGFO contract, the insurer receives a premium, but later reimburses the insured a certain amount of money each time the insured suffers a qualified financial loss as defined by the IGFO contract terms.

There are several variables of an IGFO contract that are usually determined through negotiation. For example, both parties may stipulate a certain deductible forced outage capacity and a deductible strike price, as well as a total limit of reimbursement.¹ Such variables are called negotiable variables.

Usually there are two conditions that must be met in order for the insured to receive an insurance payout during the IGFO covered period:

1. the amount of GFO capacities exceeds the amount of stipulated deductible capacity; and

¹In practice, one party, usually the buyer will initiate a set of such desired variables.

2. the market prices during the outage period are above the stipulated strike price.

If the time value of money is ignored, the expected value of the IGFO payouts to the insured is:

$$I = E[\min[C, \sum_{t=1}^N \max(\sum_{j=1}^M Q_t^j - K_q, 0) \times h \times \max(p_t - K_p, 0)] - p] \quad (4.1)$$

where,

E : the expected value operator;

C : the payment cap (maximum payment from the insurer);

Q_t^j : the outage capacity of generator j in period t ;

K_q : the deductible capacity. The insurer will pay the insured only for total outage capacity that is higher than this deductible capacity;

p_t : the spot market price during period t ;

K_p : the strike price. The insurer will pay the insured only if the spot market price is higher this strike price K_p ;

N : the contract period of insurance, e.g. number of days;

M : the number of generators under the IGFO insurance coverage;

h : the number of hours of the day (usually $h = 16$ if only peak hour power generation is of interest);

p : the insurance premiums.

When evaluating an IGFO contract, we first initiate a mathematical description of the insurance structure, a model of the insured's utility function, models of non-negotiable input factors (e.g. electricity spot market prices, generators forced outage, etc.), and identifies the negotiated variables (strike price, deductible capacity, payment cap, etc.).

Since the payout distribution of an IGFO is usually asymmetric because of its double-trigger option structure. In general, due to the complexities of the involved non-negotiable input factors, e.g. electricity price movements and GFO processes, the IGFO payout distribution cannot be calculated analytically. Consequently, the value of an IGFO payout has to be obtained through numerical methods. Simulation software such as Microsoft(R) Excel based @Risk can be utilized for simulation.

Non-negotiable variables are usually modeled as random variables, so they can be either directly calculated with given preprogrammed stochastic processes, or they might be input from other modeling packages. For example, [11] puts forward some structural models of spot market prices that might be interfaced with this simulation process to generate spot prices.

4.3 Optimal Choice of Feasible IGFO Structure

In this section we first discuss the definition of FSI. Then we present the calculation of FSI to identify feasible IGFO structures. Finally we briefly show how to select the optimal IGFO structure after quantifying FSI.

4.3.1 Definition

One of the fundamental assumptions of the utility maximization based evaluation framework for IGFO contracts is that the insured will seek optimal negotiated variables, including deductible GFO capacity and strike price, which maximize its utility by achieving an optimal trade off between paid IGFO premium and insured GFO risks. Such assumption also holds for the insurer. That is, the insurer itself needs to achieve the optimal trade-off between collected insurance premium and insured GFO risks.

Without loss of generality, we assume the risk preference of the insured or the insurer can be represented by one certain form of utility function. In this chapter we adopt the quadratic utility function as in [57]:

$$U(\mu, \sigma, \tau) = \mu - \frac{\sigma^2}{\tau} \quad (4.2)$$

where

μ : the expected return (profit/loss);

τ : the risk tolerance coefficient;

σ : the standard deviation of the return (profit/loss).

In general, the GFO process (amounts and frequency) and electricity market prices are assumed to be exogenous variables. Therefore, for a certain IGFO structure, i.e. for an already determined particular set of values for the negotiated parameters, the expected profit/loss μ , as well its standard deviation σ are functions of the insurance premium p . In other words, the

insurance premium decides the utility of the IGFO contract after its negotiated parameters are fixed. The higher the premium is, the lower the utility.

From the perspective of certainty equivalence (CE), when evaluating an IGFO contract, the EUC will compare the utility gained from paying insurance premium upfront for covering future risks, namely $U_{insured}(P)$, versus $U_{insured}^0$, which is the utility of other available hedging approaches such as entering into a long term electricity purchasing contracts, self-insurance or buying call options [105]. The upper bound of the premium $\bar{P}_{insured}$ that the EUC is willing to pay is given by the solution to (4.3). If the price of an IGFO contract is higher than $\bar{P}_{insured}$, the insured will not purchase an IGFO.

$$U_{insured}(\bar{P}_{insured}) = U_{insured}^0 \quad (4.3)$$

On the other hand, the insurer will also compare $U_{insurer}(P)$, which is the utility gained from getting the insurance premium now and payouts later to the insured, with the utility of not getting the business, or $U_{insurer}^0 = 0$. By equating these two utilities the minimum purchasing price $\underline{P}_{insurer}$ can be derived as the solution to (4.4). That is, the insurer will rather not have the business if the premium that the insurer is able to collect is lower than $\underline{P}_{insurer}$.

$$U_{insured}(\underline{P}_{insurer}) = U_{insurer}^0 = 0 \quad (4.4)$$

The feasibility structure index, or FSI, of IGFO, is hereby defined as the price difference between $\bar{P}_{insured}$ and $\underline{P}_{insurer}$. It is an indicator of whether such an IGFO contract can possibly be completed or not. If FSI is positive, it indicates that the IGFO contract is possible to be settled. Consequently, the IGFO

structure is deemed *feasible*. Otherwise, an IGFO contract is *infeasible* and can never be completed.

4.3.2 Decomposition of Payout Distribution

By adopting the quadratic form utility function in (4.2), we assume the normal distribution of the payout distributions. Therefore, we search for two normal distributions that, when weighted appropriately, best approximate the original asymmetric payout distributions from the simulation. The output is a vector of values $\theta = (\mu_1, \sigma_1, \mu_2, \sigma_2, \omega)$ that corresponds to the parameters of the approximating normal distributions (μ, σ) and the weighting factor ω .

Although closed form solutions to the decomposition problem can sometimes be found [56], [4], [89] and [90], in general they do not exist. To generalize the evaluation model, a numerical method based upon Maximum Likelihood Estimation (MLE) is chosen for decomposing the original receipt distribution into a mixture of two normal distributions. This is done by solving the problem in (4.5) below to calculate the elements of θ and the solution is the input to the utility maximization.

$$\min \sum_{i=1}^J \left[\bar{L}_i - \left(\frac{\omega}{\sqrt{2\pi\sigma_1^2}} e^{-\frac{(p_i - \mu_1)^2}{2\sigma_1^2}} + \frac{1 - \omega}{\sqrt{2\pi\sigma_2^2}} e^{-\frac{(p_i - \mu_2)^2}{2\sigma_2^2}} \right) \right]^2 \quad (4.5)$$

4.3.3 Feasible Structure

According to [58] and as we have just shown, the IGFO contract payout distribution can be approximated by decomposing it into two independent

normal distributions with proper weights. This decomposition enables us to calculate the feasible structure index (FSI) analytically.

Assuming the premium required for a certain IGFO contract is p as in (4.5), the insured has an expected profit of $\omega(\mu_1 - p)$ for the first decomposed approximating payout distribution and $(1 - \omega)(\mu_2 - p)$ for the second payout distribution. The utility of the insured can be obtained using (4.6):

$$U(P) = -p + \left[\omega\left(\mu_1 - \frac{\sigma_1^2}{\tau_1}\right) + (1 - \omega)\left(\mu_2 - \frac{\sigma_2^2}{\tau_1}\right) \right] \quad (4.6)$$

where τ_1 is the risk tolerance coefficient for the insured.

From (4.3), the upper bound of the price, or $\bar{P}_{insured}$, that the insured is willing to pay for the IGFO contract, can be calculated by (4.7):

$$\bar{P}_{insured} = \left[\omega\left(\mu_1 - \frac{\sigma_1^2}{\tau_1}\right) + (1 - \omega)\left(\mu_2 - \frac{\sigma_2^2}{\tau_1}\right) \right] - U_{insured}^0 \quad (4.7)$$

On the other hand, for the insurer, given an IGFO contract premium p , its utility will be:

$$U(p) = p - \left[\omega\left(\mu_1 + \frac{\sigma_1^2}{\tau_2}\right) + (1 - \omega)\left(\mu_2 + \frac{\sigma_2^2}{\tau_2}\right) \right] \quad (4.8)$$

where τ_2 is the risk tolerance coefficient for the insurer.

Since $U_{insurer}^0 = 0$ for the case where the insurer does not sell the IGFO contract, according to (4.4), the minimum selling price $\underline{P}_{insurer}$ that makes the insurer indifferent from selling the IGFO contract can be calculated by

$$\underline{P}_{insurer} = \omega\left(\mu_1 + \frac{\sigma_1^2}{\tau_2}\right) + (1 - \omega)\left(\mu_2 + \frac{\sigma_2^2}{\tau_2}\right). \quad (4.9)$$

FSI can then be derived by subtracting (4.7) from (4.9),

$$FSI = -\frac{\tau_2 + \tau_1}{\tau_1 \tau_2} [\omega \sigma_1^2 + (1 - \omega) \sigma_2^2] - U_{insured}^0. \quad (4.10)$$

Define c as the risk tolerance contrast ratio between these two counter parties, then (4.10) becomes:

$$FSI = -\frac{1 + c}{c} \times \frac{1}{\tau_1} \times [\omega \sigma_1^2 + (1 - \omega) \sigma_2^2] - U_{insured}^0. \quad (4.11)$$

This implies that given a particular insurance structure and the risk tolerance level of the insured, the risk tolerance contrast ratio c will affect FSI. Therefore, the feasible structures are given by $FSI \geq 0$, or

$$U_{insured}^0 \leq -\frac{1 + c}{c} \times \frac{1}{\tau_1} \times [\omega \sigma_1^2 + (1 - \omega) \sigma_2^2]. \quad (4.12)$$

4.3.4 Optimal IGFO Structure

After identifying the FSI of each IGFO structure, we apply the utility maximization based framework developed in [58] for the selection of optimal IGFO structure from the identified feasible IGFO structures.

In this process, since we have found the two approximating normal distributions for the original payout distribution, the IGFO buyer's utility can be easily calculated and stored. Various sets of negotiated variables of feasible IGFO contracts will then be updated in the evaluation process until all sets of negotiated variables are updated. The optimal choice will then be the set of negotiate variable that yields the highest utility for the investor.

Since the simulated insurance payout distributions is a function of the negotiated variables, if we let Π denote this vector of negotiated variables, the optimal choice can be calculated by solving (4.13):

$$Max_{\Pi} U(\theta(\Pi)) \tag{4.13}$$

The next two sections demonstrate the concepts and the calculation of the FSI of IGFO contracts using an example of the evaluation and negotiation of a simplified IGFO contract.

4.4 Numerical Application

In this section we first present the setup in our case study application and the simulation results. We then show the FSI calculations. Finally, we show some caveats in applying our framework.

4.4.1 Case Setup and simulation results

In our application we used the same case setup as in [58] where an EUC is considering an IGFO contract to cover its seven generation units with total generation capacity of approximately 2,000 MW. The effective period of the IGFO contract is the on-peak hours (16 hours, from hour 7-22) for four consecutive months (120 days). The generation forced outage rate is assumed as 8% of the total generation capacity, or 165MW. The on-peak electricity price is modeled as a two-state model, with an average price about \$55/MWh at normal state. For simplification purposes, it is further assumed that there

is no cap for the maximum insurance payment.

Table 4.1 lists the decomposition results for each set of negotiated variables. Across the rows the strike price (K_p) ranges from \$80/MWh to \$120/MWh, with the deductible capacity (K_q) ranges from 124 MW or 6% of the total generation capacity, to 207 MW or 10% of the total generation capacity under coverage of the insurance. For illustration purposes only three capacity values and strike prices are shown.

Strike	Capacity	124 MW		
Prices	Dist.	Mean	StDev	Weight
\$80	A	\$ 744	\$ 359	46.22%
	B	\$ 1,297	\$ 516	53.78%
\$100	A	\$ 701	\$ 339	47.02%
	B	\$ 1,223	\$ 488	52.98%
\$120	A	\$ 649	\$ 318	53.73%
	B	\$ 1,138	\$ 457	46.27%
Strike	Capacity	165 MW		
Prices	Dist.	Mean	StDev	Weight
\$80	A	\$ 636	\$ 318	46.33%
	B	\$ 1,144	\$ 468	53.67%
\$100	A	\$ 588	\$ 298	55.07%
	B	\$ 1,064	\$ 440	44.93%
\$120	A	\$ 536	\$ 270	40.93%
	B	\$ 970	\$ 412	59.07%
Strike	Capacity	207 MW		
Prices	Dist.	Mean	StDev	Weight
\$80	A	\$ 527	\$ 275	43.76%
	B	\$ 983	\$ 419	56.24%
\$100	A	\$ 494	\$ 259	43.82%
	B	\$ 923	\$ 385	56.18%
\$120	A	\$ 459	\$ 242	43.75%
	B	\$ 863	\$ 371	56.25%

* all currency units are $\times \$1,000$

Table 4.1: Decomposition Results

4.4.2 Feasible IGFO Structures

In the process of deriving the upper bound of the buying price for the EUC, the base case is set to be the scenario where the EUC chooses to self-insure and not buy the IGFO product. Such assumption is simply for the illustration purposes. In actual practice, however, one will need to consider

the best available option, such as long term power purchase agreement or electricity price call option, for the base case.

The loss distribution in the base case of no insurance is decomposed into two approximating normal distributions and they are shown in Table 4.2.

Dist.	Mean	StDev	Weight
A	\$ 1,416.9	\$ 554.5	49.14%
B	\$ 2,206.5	\$ 756.1	50.86%

Table 4.2: Distribution Decomposition for Not Insured

Figure 4.1 shows the decomposition result of the original loss distribution (because of no insurance or hedging). As shown in Figure 4.1, the approximating distribution, which is a combination of two normal distributions, is very close to the original distribution.

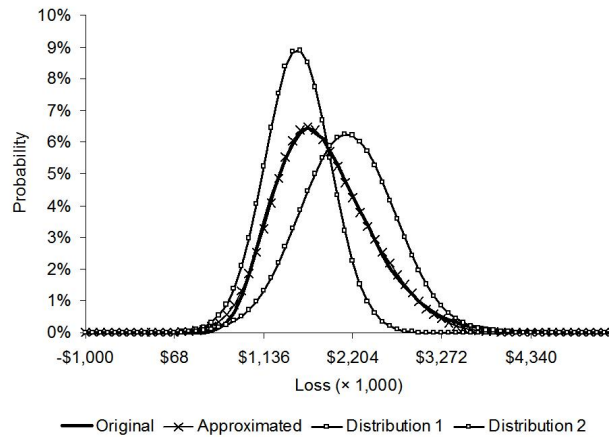


Figure 4.1: Decomposition result of an original payout distribution

The risk tolerance of the EUC is set to be \$3 million as in [58] and the

utility of no insurance is $U_{insured}^0 = -1.97 \times 10^6$ for the EUC.² The upper bound prices that the EUC is willing to pay for various IGFO structures can be calculated by solving (4.7) and are listed in Table 4.3. Table 4.4 shows the expected payout of each IGFO contract.

Deductibles	124 MW	165 MW	207 MW
\$80	\$1,121.4	\$1,000.8	\$886.9
\$100	\$1,064.5	\$904.0	\$844.6
\$120	\$972.4	\$896.4	\$799.1

Table 4.3: Upper Bound Prices of IGFO Contracts for the EUC ($\times 1,000$)

Deductibles	124 MW	165 MW	207 MW
\$80	\$1,041.8	\$908.2	\$783.6
\$100	\$977.3	\$801.9	\$734.9
\$120	\$875.4	\$792.5	\$686.2

Table 4.4: Expected Payouts of Different IGFO Contracts ($\times 1,000$)

Table 4.5 shows the probabilities that the insurance payout at each structure would exceed the upper bound of the purchase prices that the EUC is willing to pay. Such probabilities range from 35% to 41% indicating that there is less than 50% possibility that the EUC will actually *profit* from buying the IGFO contract. This reflects the nature of risk averseness of the EUC.

Deductibles	124 MW	165 MW	207 MW
\$80	41%	39%	37%
\$100	40%	37%	36%
\$120	38%	37%	35%

Table 4.5: Probabilities of IGFO Payouts to Exceed the Upper Bound Price

²Utility is a relative measure, although it is calculated based on dollar amounts. Therefore, the unit is ignored.

When assuming the insurer has the 80% of the risk tolerance level as that of the EUC, the minimum premiums required by the insurer can be calculated by solving (10) and they are shown in Table 4.6.

Deductibles	124 MW	165 MW	207 MW
\$80	\$1,126.3	\$976.6	\$838.7
\$100	\$1,052.3	\$858.4	\$781.9
\$120	\$938.2	\$846.7	\$729.1

Table 4.6: Minimum Prices of IGFO Contracts for the Insurer ($\times 1,000$)

Table 4.7 shows the FSI and the utility from IGFO payouts for all the IGFO structures considered. The first number in the cell is the FSI and the second number is the utility.

Deductibles	124 MW	165 MW	207 MW
\$80	-\$4.9, 974.1	\$24.1, 853.5	\$48.2, 739.6
\$100	\$12.3, 917.2	\$45.6, 756.7	\$62.7, 697.3
\$120	\$34.2, 825.1	\$49.6, 749.1	\$70.0, 651.8

Table 4.7: FSI and Utility for Different IGFO Contracts ($\times 1,000$)

As we can see, the one with a deductible GFO amount of 124MW and strike price of \$80/MWh has a negative FSI (\$-4,900). When FSI is negative, it indicates that the EUC is not willing to pay the enough money to the insurer for the IGFO products, even when its utility is high (974,100). Usually it happens when the strike price is low and/or in this case, the deductible GFO amount is low and the contract is *in-the-money* so that the payout probability is high. This is making sense since buying in-the-money option means buying some intrinsic value, which can be achieved by buying forward outright. Insurance product, by definition, are designed for mitigating events with low probability of occurrence but unbearable risks for the insured. Therefore, an

EUC should normally purchase an *out-of-money* call option for the insurance purpose. However, it is not to say that the more out-of-money, the better, since the utility of buying an out-of-money option decrease with the degree of out-of-moneyness.

Table 4.7 also shows that FSIs widen as the deductibles increases. The rationale is as follows. By the definition of the IGFO contract, as the deductibles increase, it becomes less likely for an IGFO payout to be paid out (or received). Therefore, the risk averseness of these two counter parties will play key roles in determining if a transaction can be completed or not. For example, if the insurer perceives less risk than the insured does, the insurer may be willing to charge less in order to get the business while the insured may be willing to pay more in order to hedge the risks. This is consistent with the observation in Table 4.5 where the insured are highly risk averse.

4.4.3 Caveats

As pointed out in [58], for simplification purpose, we assume these generators are price takers, which means their outages do not impact the electricity spot price. In actual practice, strong correlation between GFO and electricity price does exists once the system-wide GFO exceeds a certain threshold [25] and it should be taken into account in modeling effort.

It is also assumed that no generator gaming is considered. Discussions on how relaxing these assumptions will affect IGFO evaluation may be an interesting topic for the future research, especially in LMP markets. Another

assumption of interactions the counterparties is their independency, i.e. observing the counterparty's risk preference will not impact a decision maker's own risk tolerance level. These two assumptions should be carefully examined in the actual practice.

Finally, it is worth pointing out that due to the illiquid IGFO market, the application and extension of the framework presented in this section requires extra caution and validation.

4.5 Factors Affecting FSI

In this section, we study three factors that could possibly affect FSI. They are *risk tolerance contrast ratio*, *price spikes*, and *insurance aggregation*. Detailed analysis are as follows.

4.5.1 Risk Tolerance Contrast Ratio

The risk tolerance coefficient, τ , of a firm reflects its risk tolerance level. A company with higher risk tolerance level is more likely to accept riskier projects than one with lower risk tolerance. The risk tolerance level of a company could be estimated through certain public information such as 10-k filings. An example of such calculation in the petroleum E&P firms can be found in [99].

The risk tolerance contrast ratio, $c = \tau_{insurer}/\tau_{insured}$, therefore reflects the difference of risk averseness between these two IGFO counter parties. When we increase the risk tolerance level contrast ratio between the

insurer and the insured from 0.5 to 10, we are effectively switching the *relative risk preference* of the insurer from being somewhat conservative to being very aggressive.

Table 4.8 shows the FSI for different IGFO contracts when the risk tolerance ratio is 0.5 (the insurer is more conservative than the insured) instead of 1 (the insurer and the insured have the same risk preference) as in the previous example in Section IV.

Deductibles	124 MW	165 MW	207 MW
\$80	-\$55.7	-\$16.9	\$15.2
\$100	-\$32.8	\$1.1	\$30.1
\$120	-\$11.5	\$17.1	\$44.2

Table 4.8: FSI for Different IGFO contract ($\times 1,000$)

In contrast to the results in Table 4.7, the results in Table 4.8 show that almost half of these contracts are infeasible since insurer's minimum selling price is higher than the insured's maximum buying price due to insurer's low risk tolerance. The FSI for the feasible structure a very tight range of only \$1,100 for the one with 165 MW capacity deductible and \$100/MWh price deductible. Table 4.8 also shows the maximum FSI becomes \$44,200, down from the \$70,000 shown in Table 4.7, indicating the insured will benefit from seeking IGFO contract from an insurer with larger risk tolerance level, which is consistent as (4.10) indicates. Figure 4.2 shows the maximum FSI as risk tolerance contrast ratio varies from 0.5 to 10.

In Figure 4.2, we can see that the value of the FSI increases from \$44,200 to about \$110,000 as the risk tolerance contrast ratio increases from

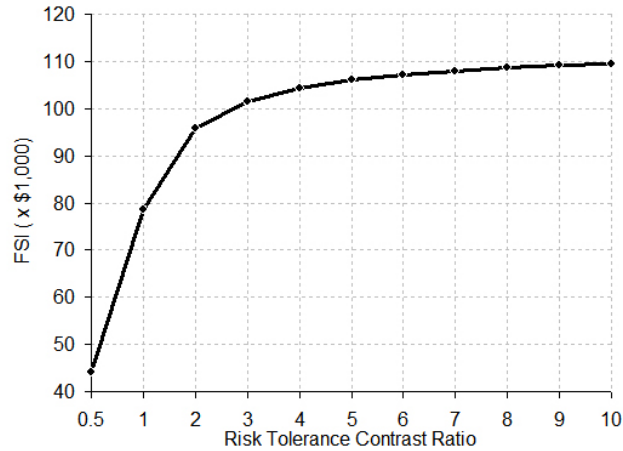


Figure 4.2: Maximum FSIs as a function of risk tolerance contrast ratio

0.5 to 10. This result indicates that, in terms of FSI, the EUC benefits from buying IGFO contracts from insurance companies who are willing to take more risks because the insurance premium will be more aggressively priced than that priced by a more risk averse insurer. However, the benefit gradually levels out once the risk tolerance ratio exceeds 2.

4.5.2 Price Volatilities

Since high electricity price is one of the payout triggers for an IGFO contract and is assumed to be exogenous, this section studies the impact of price spikes on the IGFO feasible solutions.

Figure 4.3 compares the FSI of the base case with a scenario of higher probability of price jumps.

The case of higher probability of price jumps shows similar trend to the

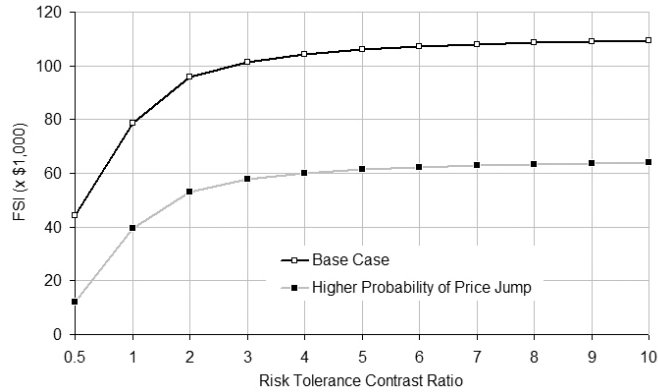


Figure 4.3: FSIs at different price jump probability

base case as the risk tolerance contrast ratio increases, but has much smaller FSI. This indicates less feasible structures exist if the supply/demand in the electricity market becomes tighter and more frequent price spikes are expected.

4.5.3 Insurance Aggregation

It is possible for the insured to provide more than one IGFO insurance contract to multiple buyers during the same time horizon, or for that matter, for the insured to purchase IGFO for its generators separately or as a bundle. This section shows how such insurance aggregation could affect FSI.

The study is simplified by duplicating the EUC studied in our application, i.e. both firms have identical generation portfolios. We calculate the FSI of the IGFO contract when these two EUCs form an alliance to pursue a new IGFO contract that has the same structure as the one each individual would select. Figure 4.4 shows the FSI of the aggregated IGFO contract.

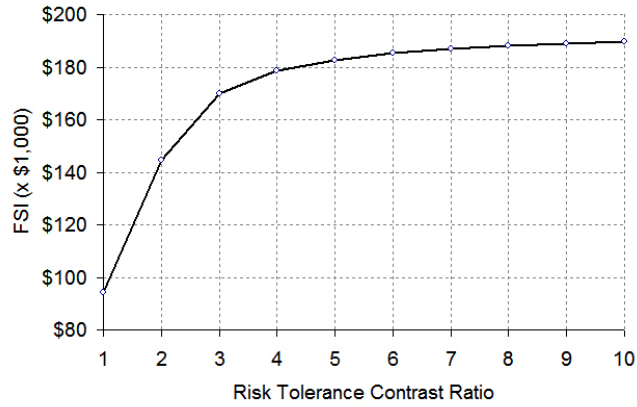


Figure 4.4: FSI of the aggregated IGFO contract

It shows that the FSI of the aggregated IGFO contract has a similar pattern to the single IGFO contract in Figure 4.2, i.e. the feasible structures increase as the risk tolerance contrast ratio increases.

Figure 4.5 compares the FSI of the aggregated IGFO contract with that of a single IGFO contract, which we define as the *aggregation ratio*.

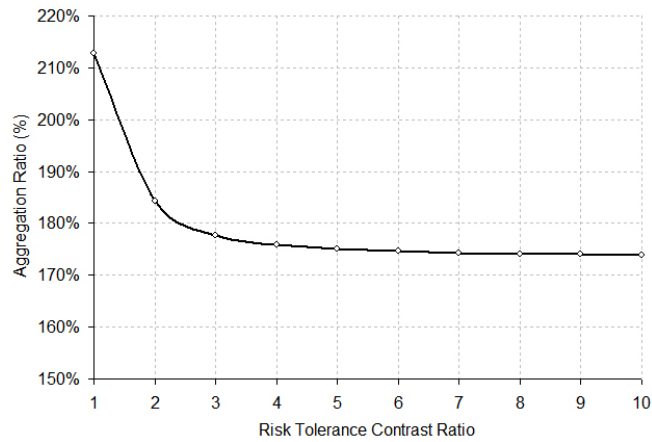


Figure 4.5: Aggregated ratio when replicating IGFO contracts

It shows that the FSI of insuring two firms is not simply double of that of a single contract, which should yield an aggregation ratio of 2. Instead, the aggregation ratio actually decreases monotonically to be below 2 as the risk tolerance contrast ratio increases to be greater than about 1.4.

This result should hold in general because when aggregating IGFO contracts for two or more generation portfolios, the risk profile of each portfolio are pooled together and the risk profiles of the aggregated contract would become easier to be quantified. For example, consider the case where hundreds of generation portfolios are aggregated. As a result, decision making becomes less subjective than in the individual scenario and therefore effectively narrows the FSI.

In this simplified example, the aggregation ratio being lower than 2 implies that even though the absolute FSI increases as shown in Figure 4.4, the FSI narrows relatively once the risk tolerance ratio gets higher. Therefore, in terms of FSI, the EUC is better off aggregating the IGFO contracts of two generation portfolios if the risk tolerance contrast ratio is lower than 1.4 because it gains relatively greater FSI (210% of the FSI of not aggregating), otherwise it should separate them.

4.6 Conclusions

In this chapter we studied the FSI of the IGFO contract between EUCs (the insured) and the insurer, which is important to identify the feasibility of an IGFO contract. By utilizing the distribution approximation theory to

approximate the asymmetric distribution of insurance receipts, we present the analytical formulations of the upper bound of the FSI of an IGFO contract. Through FSI, we can identify feasible structures of IGFO contracts, the optimal IGFO structure is than the feasible structure that maximizes insured's utility function. FSI is affected by the risk tolerance ratio of the insurance company over the insured. We also show that the FSI will narrow if price spikes are more likely to happen. Finally, we show that when EUCs bundle their IGFO contracts, the effective FSI narrows while the absolute FSI increases as individual IGFO contract does.

Chapter 5

Conclusions and Future Research

In this section we first summarize the research we presented in this dissertation, we then lay out the potential future research stemming from this dissertation.

5.1 Summary of Current Results

In this dissertation we studied some issues related to the integrated risk management in EUCs, proposed two integrated risk management frameworks for EUCs in deregulated electricity markets and most importantly, showed the successful integration and application of utility theory in this area, which has been proved to be useful in actual practice.. This dissertation presented research on certain fundamental factors in risk management in the electric power industry, together with a study on the correlation between two fundamental factors, in Chapter 2. Then an optimal natural gas supply framework for EUCs is proposed in Chapter 3. Finally, the feasible structure index (FSI) of an IGFO contract are defined in Chapter 4 with an application.

In Section 2.1 we proposed a knowledge-based statistical model to forecast weather sensitive electricity load. We have shown that incorporating

knowledge-based weather segmentation can improve forecast accuracy. The model has been integrated into the energy management system (EMS) of the Lower Colorado River Authority, Austin, TX. In Section 2.2 we presented an empirical study on electricity spot price dynamics, which distinguished the impact of system-wide generation forced outage. Result of the research has been incorporated to a successful modeling of ERCOT electricity spot price. In Section 2.3 we studied the correlation between natural gas price and electricity demand in ERCOT area.

In Chapter 3 has presented an integrated risk management framework for optimizing natural gas supply for EUCs who own and operate natural gas fired power plants (NGFPP). This framework has been the first optimization model in solving such optimal supply mix problems by systematically integrating and modeling various risk factors and constraints. Unlike traditional cost-minimization approaches, this novel framework aims to maximize utility for EUCs and achieve optimal cost-risk balance, which is the essence of integrated energy risk management, but is missed in traditional approaches.

Chapter 4 has introduced a scheme for EUCs to investigate the feasible structures of insurance on generation forced outages (IGFO). A general framework was proposed to facilitate analysis of FSI of an IGFO contract. In Chapter 4, several key factors and behaviors that may impact the FSI have been identified. The future research, based on the proposed framework, is to quantify their impacts in details.

5.2 Integrated Risk Management Framework

The research presented in this dissertation contributes to the literature of integrated risk management for EUCs, which is a new area in the power system economics in the light of the emerging electricity market deregulation. It is an inter-disciplinary area which requires the combined knowledge of power system engineering, financial engineering, and economic analysis.

This section reviews the transition of EUCs' operation perspectives from the traditional approach under the regulated environment to the current integrated risk management framework. We will present some discussions and potential research in this area in the next section.

5.2.1 Traditional Approach

Traditionally the operations and planning of EUCs were mostly centered around the reliability constrained cost minimization analysis with very little, if any, attention to the impact on their financial risk consequences.

There were two objectives under the regulated environments. The primary objective was to ensure the power system reliability, which usually was met by setting a certain reserve margin, e.g. 15% of the load obligation. The second objective then was to focus on minimizing the total costs.

Figure 5.1 shows the decision making process for EUCs in the regulated markets. As we have discussed in the Introduction of the dissertation, these two objectives were mainly due to the then regulated rate of return mecha-

nism. EUCs were not motivated to worry about their levels of competence or managing their financial risk exposures.

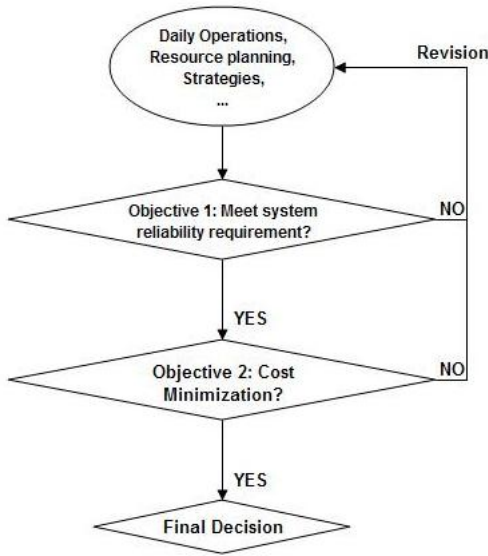


Figure 5.1: Traditional approach

5.2.2 Transition to Deregulation Markets

As the electricity industry experienced deregulation, many new issues have emerged during the transitions. The traditional regulated rate of return is no longer guaranteed, causing most EUCs to switch their focus from the traditional cost minimization.¹ Integrated risk management has gradually become a standard practice for EUCs in deregulated electricity markets. The reliability of the electricity system arguably still remains as the first priority

¹In some cases, such as in Texas, utility cooperatives and municipal-owned can choose not to opt-in the deregulation.

for EUCs. However, the secondary objective has now become to meet a certain risk related objective instead of the traditional objective of cost minimization.

In competitive electricity markets, EUCs have to establish and position themselves as competitively as possible in order to survive, not to mention grow. As the markets exhibit tremendous volatilities, cost minimization has become a secondary issue compared to optimal risk management as no EUC can afford the possible catastrophic outcomes of a risky decision.

Integrated risk management framework is a solution that has been gradually recognized and applied by EUCs to achieve the optimal risk/cost balance and tackle this objective. The essential feature of an integrated risk management framework is for an EUC to identify one or more critical risk factors that matter the most to the EUC and to position itself into a comfortable risk zone. Figure 5.2 shows this transition.

The transition from the objective of minimizing cost into the objective of optimal risks taking is in fact a natural transition. When risks are present, the fundamental of risk management is to achieve the optimal balance between the risk exposures and costs. In other words, sound risk management requires an EUC to be able to manage the risk exposure to a level that allows the EUC to explore opportunities, but not to spend too much on mitigating risks, or hedging.

In regulated environments, there was no risk for EUCs to worry about. Apparently, the objective was then to minimize the costs. However, as the

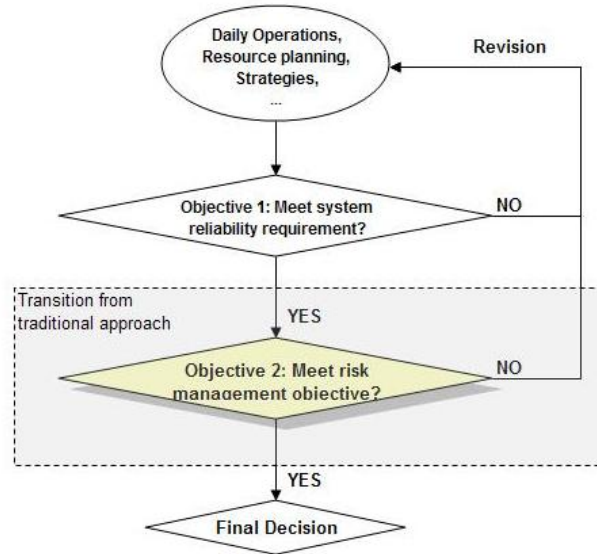


Figure 5.2: Transition from traditional approach

electricity markets experienced deregulation and the impacts of risk exposures become huge, the switch to the consideration of risks is inevitable.

5.2.3 Utility Maximization Based Framework

We have proposed several utility maximization based integrated risk management models for EUCs and described their application in EUCs in this dissertation. The underlying concept was to achieve the goal of an optimal, consistent, and true integrated risk management framework for EUCs by centering decision making on maximizing EUCs management's utility.

In fact, in the regulated environment, EUCs have been maximizing their utility by minimizing the costs because there were essentially no risks born by the EUC at all: their customers bore all the risks! Referring to the transfor-

mation of classic return-risk framework to cost-risk framework in Section 3.3, cost minimization was exactly the best and only solution then. Decision making was centered on this solution and was consistent with maximizing EUCs management’s utility in a sense. In deregulated markets, incorporating risks in the utility maximization process has become a natural transition from the traditional cost minimization method. Figure 5.3 outlines the unified framework and its different best practice before and after deregulation.

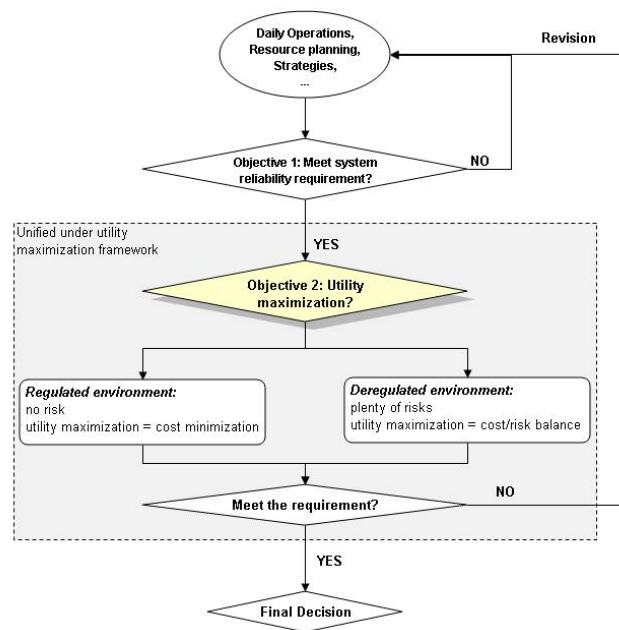


Figure 5.3: Unified integrated risk management framework

However, one major difference in the practice of deregulated markets is the constant evolving risk monitoring and analysis. This is because in regulated environments, once a decision has been made based on the expected cost minimization framework, there was not much variance considered when car-

rying it out. However, in deregulated electricity markets, as various uncertain variables change over time, a constant review, analysis, and response to these changes has become a necessity.

Figure 5.4 shows what are inside the utility maximization framework in deregulated environments with some of the models and applications that we presented in the previous chapters of this dissertation.

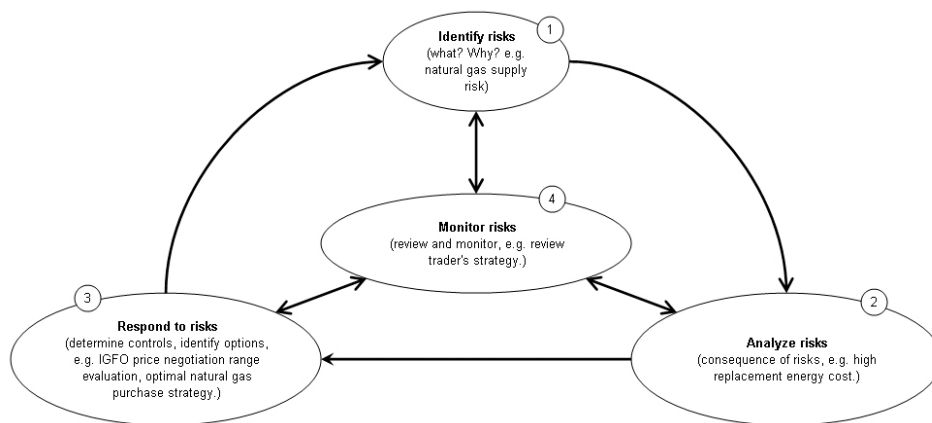


Figure 5.4: Integrated risk management practice

In Figure 5.4, four major components centering around risks consist of the integrated risk management for EUCs. There are three components that are executed by orders. When a risk is identified (component 1), it needs to be analyzed (component 2), then it is to be responded (component 3). Meanwhile, a risk monitor mechanism (component 4) is in place to review and monitor the risks continuously. For example, in Figure 5.4, the natural gas supply risk is first identified. Then the consequence of the risk, e.g. the risk of high replacement energy cost, is analyzed. After that, an optimal natural

gas purchase strategy is developed to respond to this risk. Meanwhile, the risk monitor mechanism is in place to continuously review and monitor the practice, which in this case is the current trader's strategy.

5.3 Future Research

We have presented several novel, but limited integrated risk management models for EUCs in this dissertation. There is much work to be done to expand their application as deregulated electricity markets evolve. This section identifies current limitations and future research for the integrated risk management framework proposed in this dissertation and other issues.

5.3.1 Integrated Risk Management Framework

Running an EUC requires complicated interacting operations and decision making. By centering these operations and decision makings with a unified utility maximization based risk management framework, we hope to achieve optimal risk exposure consistently throughout the operations, which is the best practice of risk management.

Figure 5.5 shows an example integrated risk management framework in decision making process for an EUC. By applying utility maximization models in solving problems 1 through 7, we are sure that the EUC is able to achieve optimal cost-risk balance in every decision making process separately, and consequently, we hope to achieve an enterprise-wide optimal cost-risk balance for the EUC on a consistent basis.

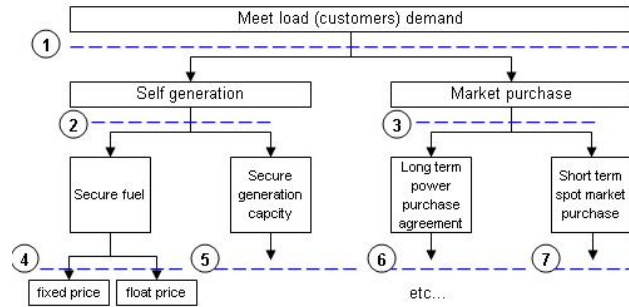


Figure 5.5: Example of a framework

There are limitations for the utility maximization based integrated risk management framework we proposed. These limitations suggest the following two major limits are identified and listed as follows, along with suggested future research.

First, the framework is based on the assumption that a single utility function is sufficient to represent the risk preference of the EUC management. The utility function, including its form and parameters, are currently arbitrary and prone to estimation errors. Future research should include analysis of the impacts due to the inaccuracy of the utility function estimation. In other words, the estimation of the EUC management has potentially become a built-in risk factor for the integrated risk management framework and needs to be analyzed in the future. This will be a very challenging task.

Second, we are assuming relative independence of decision makings as we are seeking the enterprise wide utility maximization by optimizing each decision making process separately (such as decision making processes 1-7 in

Figure 5.5). In other words, we are solving the sub-optimal problems and combining these parallel solutions as an overall solution. If there is no correlation amongst the various decision making processes, then we have found an overall optimal solution. The assumption of no correlation, however, should be relaxed if *marked* correlations exist among various decision making processes. This very much deserves an intensive investigation.

5.3.2 Other Issues

A few example of other potential future research topics include:

- Integrate the concept of knowledge based segmentation we developed in Chapter 2 to modern intelligence systems such as Artificial Neural Network Models.
- Extend the two critical power system price indexes (SLCR and SGFO) we developed in Chapter 2 to the price modeling of mid/short- term to real-time applications.
- The correlation between the natural gas price and electricity demand we presented in Chapter 2 may have an impact on the modeling and pricing of energy products such as heat rate options and may deserve attentions from this perspective.
- Extend the research in Chapter 3 to study the effect of the changes or estimation errors of the risk preferences of the EUCs management. This

could lead to better understanding and application of utility theory in the integrated risk management modelings for EUCs.

- Extend the research in Chapter 4 to refine the pricing and negotiation strategy for EUCs.

Appendix

Appendix 1

Visual C++ Code for IGFO Simulator

```
#include "stdafx.h"

#include "Real Simulation.h"

#include "Real SimulationDlg.h"

#include "math.h"

#ifdef _DEBUG

#define new DEBUG_NEW

#undef THIS_FILE

static char THIS_FILE[] = __FILE__;

#endif

// CAboutDlg dialog used for App About

const float Const_Lstar = 0.823f;

const float Const_OutageRate = 0.1f;

const float de_cap = 0.2 * 2065;

const float Const_Strike = 30.0f;

const float Const_Increase = 0.0f;
```

```

//this parameter is for the control of total baseload

float percentage = 0.80f;
float permitted_outage = 2065*(1-percentage);
const float production_cost = 30.0f;
const float liquidity = 0.15*2065;

float Max(float a, float b);
void Normal(float mean, float std, int amount);
void market_price();
void load(float a, float b, float stdev, float baseload);
void load_markov(float lambda, float miu);
void payoff(float strikeprice, float outage);

float tempe[20000][120];
float de_ca[20000][120];
float pricedata[20000][120];
int markov[20000][120];
float loaddata[20000][120];

float temp_random[20000];
float totalpayoff[20000];

```

```

void histogram(int interval);

int trials = 20000;

class CAboutDlg : public CDialog
{
public:
CAboutDlg();

// Dialog Data
//{{AFX_DATA(CAboutDlg)
enum { IDD = IDD_ABOUTBOX };
//}}AFX_DATA

// ClassWizard generated virtual function overrides
//{{AFX_VIRTUAL(CAboutDlg)
protected:
virtual void DoDataExchange(CDataExchange* pDX);
// DDX/DDV support
//}}AFX_VIRTUAL

// Implementation
protected:
//{{AFX_MSG(CAboutDlg)

```

```

//{{AFX_MSG
DECLARE_MESSAGE_MAP()

};

CAboutDlg::CAboutDlg() : CDialog(CAboutDlg::IDD)
{
//{{AFX_DATA_INIT(CAboutDlg)
//}}AFX_DATA_INIT
}

void CAboutDlg::DoDataExchange(CDataExchange* pDX)
{
CDialog::DoDataExchange(pDX);
//{{AFX_DATA_MAP(CAboutDlg)
//}}AFX_DATA_MAP
}

BEGIN_MESSAGE_MAP(CAboutDlg, CDialog)
//{{AFX_MSG_MAP(CAboutDlg)
// No message handlers
//}}AFX_MSG_MAP
END_MESSAGE_MAP()

```

```

////////////////////////////////////
// CRealSimulationDlg dialog

CRealSimulationDlg::CRealSimulationDlg
(CWnd* pParent /*=NULL*/)
: CDialog(CRealSimulationDlg::IDD, pParent)
{
//{{AFX_DATA_INIT(CRealSimulationDlg)
m_aug_a = 0.44f;
m_aug_b = 87.05f;
m_aug_s = 3.99f;
m_baseload = 60.0f;
m_jul_a = 0.45f;
m_jul_b = 89.98f;
m_jul_s = 2.50f;
m_jun_a = 0.42f;
m_jun_b = 88.01f;
m_jun_s = 3.54f;
m_load_a = 0.2f;
m_load_b = 46.36f;
m_load_s = 4.95f;
m_markov_00 = 0.563f;
m_markov_01 = 0.437f;
}
}

```

```

m_markov_10 = 0.563f;
m_markov_11 = 0.437f;
m_sep_a = 0.42f;
m_sep_b = 88.01f;
m_sep_s = 3.54f;
m_outage = 0.06f;
m_strike = Const_Strike;
m_trials = 20000;
m_h_interval = 300;
//}}AFX_DATA_INIT
// Note that LoadIcon does not require a subsequent
//DestroyIcon in Win32
m_hIcon = AfxGetApp()->LoadIcon(IDR_MAINFRAME);
}

void CRealSimulationDlg::
DoDataExchange(CDataExchange* pDX)
{
CDialog::DoDataExchange(pDX);
//{{AFX_DATA_MAP(CRealSimulationDlg)
DDX_Text(pDX, IDC_Aug_a, m_aug_a);
DDX_Text(pDX, IDC_Aug_b, m_aug_b);
DDX_Text(pDX, IDC_Aug_S, m_aug_s);

```

```
DDX_Text(pDX, IDC_Baseload, m_baseload);
DDX_Text(pDX, IDC_Jul_a, m_jul_a);
DDX_Text(pDX, IDC_Jul_b, m_jul_b);
DDX_Text(pDX, IDC_Jul_S, m_jul_s);
DDX_Text(pDX, IDC_Jun_a, m_jun_a);
DDX_Text(pDX, IDC_Jun_b, m_jun_b);
DDX_Text(pDX, IDC_Jun_S, m_jun_s);
DDX_Text(pDX, IDC_Load_a, m_load_a);
DDX_Text(pDX, IDC_Load_b, m_load_b);
DDX_Text(pDX, IDC_Load_S, m_load_s);
DDX_Text(pDX, IDC_Markov_00, m_markov_00);
DDX_Text(pDX, IDC_Markov_01, m_markov_01);
DDX_Text(pDX, IDC_Markov_10, m_markov_10);
DDX_Text(pDX, IDC_Markov_11, m_markov_11);
DDX_Text(pDX, IDC_Sep_a, m_sep_a);
DDX_Text(pDX, IDC_Sep_b, m_sep_b);
DDX_Text(pDX, IDC_Sep_S, m_sep_s);
DDX_Text(pDX, IDC_Outage, m_outage);
DDX_Text(pDX, IDC_Strike, m_strike);
DDX_Text(pDX, IDC_Trials, m_trials);
DDX_Text(pDX, IDC_Hist_Interval, m_h_interval);
//}}AFX_DATA_MAP
}
```

```

BEGIN_MESSAGE_MAP(CRealSimulationDlg, CDialog)
//{{AFX_MSG_MAP(CRealSimulationDlg)
ON_WM_SYSCOMMAND()
ON_WM_PAINT()
ON_WM_QUERYDRAGICON()
//}}AFX_MSG_MAP
END_MESSAGE_MAP()

////////////////////////////////////
// CRealSimulationDlg message handlers

BOOL CRealSimulationDlg::OnInitDialog()
{
CDialog::OnInitDialog();

// Add "About..." menu item to system menu.

// IDM_ABOUTBOX must be in the system command range.
ASSERT((IDM_ABOUTBOX & 0xFFFF) == IDM_ABOUTBOX);
ASSERT(IDM_ABOUTBOX < 0xF000);

CMenu* pSysMenu = GetSystemMenu(FALSE);

```

```

if (pSysMenu != NULL)
{
    CString strAboutMenu;
    strAboutMenu.LoadString(IDS_ABOUTBOX);
    if (!strAboutMenu.IsEmpty())
    {
        pSysMenu->AppendMenu(MF_SEPARATOR);
        pSysMenu->AppendMenu(MF_STRING, IDM_ABOUTBOX, strAboutMenu);
    }
}

// Set the icon for this dialog.
//The framework does this automatically
// when the application's main window is not a dialog
SetIcon(m_hIcon, TRUE); // Set big icon
SetIcon(m_hIcon, FALSE); // Set small icon

// TODO: Add extra initialization here

return TRUE;

// return TRUE unless you set the focus to a control
}

```

```

void CRealSimulationDlg::
OnSysCommand(UINT nID, LPARAM lParam)
{
if ((nID & 0xFFFF) == IDM_ABOUTBOX)
{
CAboutDlg dlgAbout;
dlgAbout.DoModal();
}
else
{
CDialog::OnSysCommand(nID, lParam);
}
}

// If you add a minimize button to your dialog,
// you will need the code below to draw the icon.
// For MFC applications using the document/view model,
// this is automatically done for you by the framework.

void CRealSimulationDlg::OnPaint()
{
if (IsIconic())
{

```

```

CPaintDC dc(this); // device context for painting

SendMessage(WM_ICONERASEBKGND,
(WPARAM) dc.GetSafeHdc(), 0);

// Center icon in client rectangle
int cxIcon = GetSystemMetrics(SM_CXICON);
int cyIcon = GetSystemMetrics(SM_CYICON);
CRect rect;
GetClientRect(&rect);
int x = (rect.Width() - cxIcon + 1) / 2;
int y = (rect.Height() - cyIcon + 1) / 2;

// Draw the icon
dc.DrawIcon(x, y, m_hIcon);
}
else
{
CDialog::OnPaint();
}
}

HCURSOR CRealSimulationDlg::OnQueryDragIcon()

```

```

{
return (HCURSOR) m_hIcon;
}

void CRealSimulationDlg::OnOK()
{
CDialog::UpdateData(TRUE);
load_markov(m_markov_01, m_markov_10);
load(m_load_a, m_load_b, m_load_s, m_baseload);
market_price();
payoff(m_strike, m_outage);
histogram(m_h_interval);
MessageBox("Done, please check file");
CDialog::OnOK();
}

void load_markov(float lambda, float miu)
{
for(int j = 0; j < trials; j++)
{
markov[j][0] = 0;
for( int i = 1; i < 120; i++)
{

```

```

float mm = (float)rand()/RAND_MAX;
if(markov[j][i-1] == 0)
{
if(mm < lambda)
markov[j][i] = 1;
else markov[j][i] = 0;
}
if(markov[j][i-1] == 1)
{
if(mm < miu)
markov[j][i] = 1;
else markov[j][i] = 0;
}
}
}
}

void load(float a, float b, float stdev, float baseload)
{
// b = b * (1 +Const_Increase);
baseload = baseload * (1 + Const_Increase);
for(int i = 0; i < trials; i++)
{

```

```

Normal(0, 1, 120);

float mr_load = b + (float)pow(-1, rand())
* (float)rand()/RAND_MAX;

for(int j = 0; j < 120; j++)
{
loaddata[i][j] = mr_load/baseload;
mr_load = mr_load + a*(b - mr_load)
+ stdev*temp_random[j];
}
}
}

void market_price()
{
float Lstar = Const_Lstar;

float a1 = 19.42f;
float b1 = -1.62f;
float stdev1= 2.83f;

float a2 = 544.07f;
float b2 = -422.25f;
float stdev2= 44.71f;

```

```

float price[120];
//initializing data
for(int i = 0; i < trials; i++)
{
for(int j = 0; j < 120; j++)
{
if(loaddata[i][j] < Lstar)
{
Normal(0, stdev1, 1);
price[j] = a1*loaddata[i][j] + b1 + temp_random[0];
}
else
{
if(markov[i][j] == 0)
{
Normal(0, stdev1, 1);
price[j] = a1*loaddata[i][j] + b1 + temp_random[0];
}
else
{
Normal(0, stdev2, 1);
price[j] = a2*loaddata[i][j] + b2 + temp_random[0];
}
}
}
}

```

```

}
}
pricedata[i][j] = 2.5f*price[j];
//2.5 serves as a fuel factor
}
}
}

void payoff(float strikeprice, float outage)
{
FILE* temp;
temp = fopen("../data\\PAYOFF.TXT", "w");
float plants_status[7];
float plant_cap[7];
float plants_loss[7];
plant_cap[0] = 290;
plant_cap[1] = 290;
plant_cap[2] = 445;
plant_cap[3] = 140;
plant_cap[4] = 140;
plant_cap[5] = 340;
plant_cap[6] = 420;
float outagerate= Const_OutageRate;

```

```

float lambda = outage;
float miu = ((1-outagerate)/outagerate)*lambda;
//so that we keep the outage rate P

float total_cap_loss;
float payoff;
for(int i = 0; i < 7; i++)
plants_status[i] = 0;
for(i = 0; i < trials; i++)
{
float totalpay = 0.0f;
float phy_payoff=0.0f;
float phy_payoff_SUM=0.0f;
float payoff_at_80P_obiligation = 0.0f;
//opportunity cost considered
float payoff_at_80P_obiligation_SUM = 0.0f;
//opportunity cost considered
float payoff_at_80P_obiligation_NC = 0.0f;
//opportunity cost not considered
float payoff_at_80P_obiligation_NC_SUM = 0.0f;
//opportunity cost considered
for(int k = 0; k < 120; k++)
{

```

```
total_cap_loss = 0;
for(int j = 0; j < 7; j++)
{
float st = (float)rand()/RAND_MAX;
if(plants_status[j] == 0)
{
if(st < lambda)
{
plants_loss[j] = plant_cap[j];
plants_status[j] = 1;
}
else
{
plants_loss[j] = 0;
plants_status[j] = 0;
}
}
else
{
if(st < miu)
{
plants_loss[j] = 0;
plants_status[j] = 0;
}
```

```

}
else
{
plants_loss[j] = plant_cap[j];
plants_status[j] = 1;
}
}
total_cap_loss += plants_loss[j];
}
//original situation
payoff = Max(0, (total_cap_loss - de_cap))
*Max((pricedata[i][k] - strikeprice), 0)*16;
//the view from physical side,
float phypayoff = Max(0, (total_cap_loss - de_cap))
*(pricedata[i][k] - strikeprice)*16;
//the situation where 80% is considered
//the percentage is defined above.
//the first scenario, opportunity cost is considered here;
if(pricedata[i][k] > production_cost)
{
if(total_cap_loss > (1- percentage)*2065)
{
payoff_at_80P_obiligation =

```

```

(total_cap_loss -(1-percentage)*2065 + liquidity)
* (pricedata[i][k] - production_cost)*16;
}
else
{
if((2065-total_cap_loss) > liquidity)
//with liquidity and no obligation situation,
//the calculation is different

{
payoff_at_80P_obiligation = 0;
//liquidity * (pricedata[i][k] - production_cost)*16;
}
else payoff_at_80P_obiligation =
(liquidity - (2065- total_cap_loss))
* (pricedata[i][k] - production_cost)*16;

}
}
else
payoff_at_80P_obiligation = 0;
//the second scenario is considered here where
//opportunity cost is not considered here;

```

```

if (total_cap_loss > permitted_outage)
payoff_at_80P_obiligation_NC =
(total_cap_loss -permitted_outage)
* Max((pricedata[i][k] - production_cost),0)*16;
else
payoff_at_80P_obiligation_NC = 0;
//finish scenarios
totalpay += payoff;
phy_payoff_SUM += phypayoff;
payoff_at_80P_obiligation_SUM
+= payoff_at_80P_obiligation;
payoff_at_80P_obiligation_NC_SUM
+= payoff_at_80P_obiligation_NC;
}
totalpayoff[i] = payoff_at_80P_obiligation_SUM;//totalpay;
fprintf(temp, "%.2f\t", totalpayoff[i]);
fprintf(temp, "%.2f\t", phy_payoff_SUM);
fprintf(temp, "%.2f\t", payoff_at_80P_obiligation_SUM);
fprintf(temp, "%.2f\n", payoff_at_80P_obiligation_NC_SUM);
}
fclose(temp);
}

```

```

void histogram(int interval)
{
float AVGPayout = 0.0f;
if (interval > 300)
interval = 300;
FILE* histogram;
const float Const_HMax = 600000.0f;
histogram = fopen("../data\\loss_histogram.txt", "w");
int category[301];
float incr = 0;
float h_min = 0;
float h_max = Const_HMax;
float steps = (h_max - h_min)/interval;
for(int i = 0; i < interval; i++)
category[i] = 0;
for(i = 0; i < trials; i++)
{
if(totalpayout[i] == 0)
category[0]++;
else for(int k = 0; k < interval; k++)
{
if((totalpayout[i] > h_min + k*steps)

```

```

&&(totalpayoff[i] <= h_min + (k+1)*steps))
category[k+1]++;
}
AVGPayoff += totalpayoff[i];
}
AVGPayoff /= trials;
fprintf(histogram, "Interval x 10k\t");
fprintf(histogram, "%.2f\n", AVGPayoff);
for(i = 0; i < interval; i++)
{
fprintf(histogram, "%.2f\t", (h_min+i*steps)/10000);
fprintf(histogram, "%d\n", category[i]);
}
fclose(histogram);
}

float Max(float a, float b)
{
if(a > b)
return a;
else
return b;
}

```

```

void Normal(float mean, float std, int amount)
{
    srand((clock()-time(NULL))*(clock()+rand()));
    for(int i = 0; i < amount; i++)
    {
        float x1, x2, y1, w;
        static float y2;
        static int use_last = 0;
        if (use_last)
            /* use value from previous call */
            {
                y1 = y2;
                use_last = 0;
            }
        else
            {
                do {
                    x1 = 2.0f * (float)rand()/RAND_MAX - 1.0f;
                    x2 = 2.0f * (float)rand()/RAND_MAX - 1.0f;
                    w = x1 * x1 + x2 * x2;
                } while ( w >= 1.0 );
            }
    }
}

```

```
w = (float)sqrt( (-2.0f * log( w ) ) / w );  
y1 = x1 * w;  
y2 = x2 * w;  
use_last = 1;  
}  
temp_random[i] = mean+y1*std;  
}  
}
```

Bibliography

- [1] M. Adya and F. Collopy. How effective are neural networks at forecasting and prediction? a review and evaluation. *J. Forecast*, 17:481–495, 1998.
- [2] Energy Information Agency. Natural gas supply. *Department of Energy*, 2006.
- [3] Energy Information Agency. Prices model description. *Department of Energy*, 2006.
- [4] M.M. Alavi-Sereshki and C. Singh. A generalized continuous distribution and approach for generating capacity reliability evaluation and its application. *IEEE Trans. Power Systems*, 6(1):16–22, February 1991.
- [5] F. Albuyeh and J. Kumar. Decision support tools for market participants. *IEEE Trans. Power Systems*, 18(2):512–516, May 2003.
- [6] C.J. Andrews. Evaluating risk management strategies in resource planning. *IEEE Trans. Power Systems*, 10(1):420–426, February 1995.
- [7] W. Avery, G.G. Brown, J.A. Rosenkranz, and R.K. Wood. Optimization of purchase, storage and transmission for natural gas utilities. *Operations Research*, 40:446–462, 1992.

- [8] R. Baldick. The generalized unit commitment problem. *IEEE Trans. Power Systems*, 10(1):465–475, February 1995.
- [9] R. Baldick and W. Hogan. Capacity constrained supply function equilibrium models of electricity markets: Stability, non-decreasing constraints and function space iterations. *University of California Energy Institute, POWER Working Paper*, PWP-089, 2001.
- [10] R. Baldick, S. Kolos, and S. Tompaidis. Interruptible electricity contracts from an electricity retailer’s point of view: valuation and optimal interruption. *to be appear in Operations Research*, 2006.
- [11] M.L. Baughman and W.W. Lee. A monte carlo model for calculating spot market prices of electricity. *IEEE Trans. Power Systems*, 7(2):584–590, May 1992.
- [12] R. Billinton and H. Chen. Assessment of risk-based capacity benefit factors associated with wind energy conversion systems. *IEEE Trans. Power Systems*, 13(3):1191–1196, August 1998.
- [13] R. Bjorgan, C-C. Liu, and J. Lawarree. Financial risk management in a competitive electricity market. *IEEE Trans. Power Systems*, 14(4):1285–1291, November 1999.
- [14] C. Blanco and D. Soronow. Jump diffusion process: Energy price processes used for derivatives pricing and risk management. *Energy and Power Risk Management*, September 2001.

- [15] C. Blanco and D. Soronow. Mean reverting process: Energy price processes used for derivatives pricing and risk management. *Energy and Power Risk Management*, June 2001.
- [16] A.E. Bopp, V.R. Kannan, S.W. Palocsay, and S.P. Stevens. An optimization model for planning natural gas purchases, transportation, storage and deliverability. *Omega*, 24:511–522, 1996.
- [17] S. Borenstein, J. Bushnell, C. Knittel, and C. Wolfram. Trading inefficiencies in california’s electricity market. *NBER Working Papers*, W8620, 2001.
- [18] S. Borenstein, J. Bushnell, and F. Wolak. Diagnosing market power in california’s restructured wholesale electricity market. *NBER Working Paper*, W7868, 2000.
- [19] S. Borenstein, J. Bushnell, and F. Wolak. Measuring market inefficiencies in california restructured wholesale electricity market. *American Economic Review*, pages 1376–1405, 2002.
- [20] R.E. Brown and J.J. Burke. Managing the risk of performance based rates. *IEEE Trans. Power Systems*, 15(2):893–898, May 2000.
- [21] J. Butler and J.S. Dyer. Optimizing natural gas flows with linear programming. *Decision Sciences*, 30(2):563–580, Spring 1999.
- [22] J. Cabero, A. Baillo, S. Cerisola, M. Ventosa, A. Garcia-Alcalde, F. Peran, and G.O. Relano. A medium-term integrated risk management model

- for a hydrothermal generation company. *IEEE Trans. Power Systems*, 20(3):1379–1388, August 2005.
- [23] H. Chen and R. Baldick. Optimizing short-term natural gas supply portfolio. *to appear in IEEE Trans. Power Systems*, 2006.
- [24] H. Chen, Y. Du, and J.N. Jiang. Weather sensitive short-term load forecasting using knowledge-based arx models. *IEEE PES General Meeting*, pages 190–196, 2005.
- [25] H. Chen and J.N. Jiang. Empirical electricity price modeling. *Energy Risk*, pages 74–79, July 2006.
- [26] S.T. Chen, D.C. Yu, and A.R. Monghaddamjo. Weather sensitive short-term load forecast using nonfully connected artificial neural network. *IEEE Trans. Power Systems*, 7(3):1098–1105, August 1992.
- [27] T.S. Chung, Sh.H Zhang, C.W. Yu, and K.P. Wong. Electricity market risk management using forward contracts with bilateral options. *IEEE Proc.-Gener. Transm. Distrib.*, 150(5):588–594, September 2003.
- [28] R.A. Collins. The economics of electricity hedging and a proposed modification for the futures contract for electricity. *IEEE Trans. Power Systems*, 17(1):100–107, February 2002.
- [29] E.O. Crousillat, P. Dorfner, P. Alvarado, and H.M. Merrill. Conflicting objectives and risk in power system planning. *IEEE Trans. Power Systems*, 8(3):887–893, August 1993.

- [30] R. Dahlgren, C.C. Liu, and J. Lawarree. Risk assessment in energy trading. *IEEE Trans. Power Systems*, 18(2):503–511, May 2003.
- [31] Y. Dai, J. McCalley, N. Abi-Samra, and V. Vittal. Annual risk assessment for overload security. *IEEE Trans. Power Systems*, 16(4):616–623, November 2001.
- [32] D. Das and B.F. Wollenberg. Risk assessment of generators bidding in day-ahead market. *IEEE Trans. Power Systems*, 20(1):416–424, February 2005.
- [33] M. Denton, A. Palmer, R. Masiello, and P. Skantze. Managing market risks in energy. *IEEE Trans. Power Systems*, 18(2):494–502, May 2003.
- [34] A.P. Douglas, A.M. Breipohl, F.N. Lee, and R. Adapa. Risk due to load forecast uncertainty in short term power system planning. *IEEE Trans. Power Systems*, 13(4):1493–1499, November 1998.
- [35] Y. Du and X. Hu. Applying modern portfolio theory to optimal gas purchasing. *Energy Power Risk Management*, pages 51–53, May 2003.
- [36] ERCOT. <http://www.ercot.com>. *website*, as of 2006.
- [37] J.Y. Fan and J.D. McDonald. A real time implementation of short-term load forecasting for distribution power system. *IEEE Trans. Power Systems*, 9(2):988–994, May 1994.

- [38] A.N. Franzblau. *A Primer of Statistics for Non-Statisticians*. Harcourt, Brace and World, 1958.
- [39] W. Fu, J.D. McCalley, and V. Vittal. Risk assessment for transformer loading. *IEEE Trans. Power Systems*, 16(3):346–353, August 2001.
- [40] W. Fu, S. Zhao, J.D. McCalley, V. Vittal, and N. Abi-Samra. Risk assessment for special protection systems. *IEEE Trans. Power Systems*, 17(1):63–72, February 2002.
- [41] S.A. Gabriel, M.F. Genc, and S. Balakrishnan. A simulation approach to balancing annual risk and reward in retail electrical power markets. *IEEE Trans. Power Systems*, 17(4):1050–1057, November 2002.
- [42] T.W. Gedra. Optimal forward contracts for electric power markets. *IEEE Trans. Power Systems*, 9(4):1766–1773, November 1994.
- [43] R. Green and D. Newbery. Competition in the british electricity spot market. *Journal of Political Economy*, pages 929–953, 1992.
- [44] J.M. Guldmann. Supply, storage and service reliability decisions by gas distribution utilities: A chance-constrained approach. *Management Science*, 29(8):884–906, August 1983.
- [45] J.M. Guldmann and F. Wang. Optimizing the natural gas supply mix of local distribution utilities. *European J. of Operations Research*, 112:598–612, 1999.

- [46] M.T. Hagan and S.M. Behr. The time series approach to short term load forecasting. *IEEE Trans. Power Apparatus and Systems*, PWRS-2(3):785–791, August 1987.
- [47] D. H. Hartman. Forced outage insurance for electric utilities. *RISK CONSULT publications*, 2001.
- [48] B. Henning, M. Sloan, and M. de Leon. Natural gas and energy price volatility. *American Gas Foundation*, 1-2, October 2003.
- [49] S. Hesmondhalgh. Is neta the blueprint for wholesale electricity trading arrangements of the future? *IEEE Trans. Power Systems*, 18(2):548–554, May 2003.
- [50] D.E. Hinkle, W. Wiersma, and S.G. Jurs. *Applied Statistics for the Behavioral Sciences*. Houghton Mifflin Co., 1988.
- [51] H. S. Hippert, C. E. Pedreira, and R. C. Souza. Neural networks for short-term load forecasting: A review and evaluation. *IEEE Trans. Power Systems*, 16(1):44–55, February 2001.
- [52] J. Hlouskova, S. Kossmeier, S. Obersteiner, and A. Schnabl. Short-term forecasting of electricity spot prices. *OSCOGEN*, 2001.
- [53] J. Hopper. Gas storage and power prices: Inextricably linked. *Energy and Power Risk Management*, November 2002.
- [54] Bloomberg Inc. <http://www.bloomberg.com>. *website*, as of 2006.

- [55] ACE International. <http://www.acepowerandutilities.com>. *website*, as of August, 2006.
- [56] R. Jarrow and A. Rudd. Approximate option valuation for arbitrary stochastic process. *Journal of Financial Economics*, 10:347–369, 1982.
- [57] J. Jia and J.S. Dyer. A standard measure of risk and risk-value models. *Management Science*, 42(12):1691–1705, 1996.
- [58] J. Jiang, H. Chen, and M.L. Baughman. Evaluation of insurance on generation forced outages. *IEEE PES General Meeting*, 2006.
- [59] J.N. Jiang. Methods for market analysis, risk management and finance in deregulated power industry. *Ph.D. dissertation, Department of Electrical and Computer Engineering, The University of Texas at Austin, Austin, TX*, 2005.
- [60] A. Juris. Development of competitive natural gas markets in the united states. *Public Policy Journal*, April 1998.
- [61] H.R. Kassaei, A. Keyhani, T. Woung, and M. Rahman. A hybrid fuzzy neural network bus load modeling and prediction. *IEEE Trans. Power Systems*, 14(2):1867–1876, May 1999.
- [62] K. Kiesen and E. Husby. A joint state-space model for spot and futures power. *Energy Risk*, 2002.

- [63] D. Kirschen. Demand-side view of electricity markets. *IEEE Trans. Power Systems*, 18(2):520–527, May 2003.
- [64] P. Klemperer and M. Meyer. Supply function equilibria in oligopoly under uncertainty. *Econometrica*, pages 1243–1277, 1989.
- [65] C. Knittel and M. Roberts. An empirical examination of deregulated electricity prices. *University of California Energy Institute, POWER Working Paper*, PWP-087, 2001.
- [66] H. Konno and H. Yamazaki. Mean-absolute deviation portfolio optimization model and its applications to tokyo stock market. *Management Science*, 37(5):519–531, May 1991.
- [67] Z. Li. Natural gas for generation. a solution or a problem? *IEEE Power and Energy Magazine*, pages 16–21, July/August 2005.
- [68] G. Lian and R. Billinton. Operating reserve risk assessment in composite power systems. *IEEE Trans. Power Systems*, 9(3):1270–1276, August 1994.
- [69] P. Linares. Multiple criteria decision making and risk analysis as risk management tools for power system planning. *IEEE Trans. Power Systems*, 17(3):895–900, August 2002.
- [70] C.N. Lu, H.T. Wu, and S. Vemuri. Neural network based short term load forecasting. *IEEE Trans. Power Systems*, 8(1):337–342, February 1993.

- [71] L. Miranda and M. Proenca. Why risk analysis outperforms probabilistic choice as the effective decision support paradigm for power system planning. *IEEE Trans. Power Systems*, pages 643–648, 1998.
- [72] V. Miranda and L.M. Proenca. Probabilistic choice vs. risk analysis—conflicts and synthesis in power system planning. *IEEE Trans. Power Systems*, 13(3):1038–1043, August 1998.
- [73] B. Mo, A. Gjelsvik, and A. Grundt. Integrated risk management of hydro power scheduling and contract management. *IEEE Trans. Power Systems*, 16(2):216–221, May 2001.
- [74] E. Ni, P.B. Luh, and S. Rourke. Optimal integrated generation bidding and scheduling with risk management under a deregulated power market. *IEEE Trans. Power Systems*, 19(1):600–609, February 2004.
- [75] A. Pankratz. *Forecasting with Dynamic Regression Models*. New York: Wiley, 1991.
- [76] S.E. Papadakis, J.B. Theocharis, and A.G. Bakirtzis. A load curve based fuzzy modeling technique for short-term load forecasting. *Fuzzy Sets and Systems*, 135(2):279–303, April 2003.
- [77] A.D. Papalexopoulos, S. Hao, and T-M. Peng. An implementation of a neural network based load forecasting model for the ems. *IEEE Trans. Power Systems*, 9(4):1956–1962, November 1994.

- [78] A.D. Papalexopoulos and T.C. Hesterberg. A regression-based approach to short-term load forecasting. *IEEE Trans. Power Systems*, 5(4):1535–1547, September 1990.
- [79] D.S. Popovic and Z.N. Popovic. A risk management procedure for supply restoration in distribution network. *IEEE Trans. Power Systems*, 19(1):221–228, February 2004.
- [80] E.A. Radwan. Short-term hourly load forecasting using abductive networks. *IEEE Trans. Power Systems*, 19(1):164–173, February 2004.
- [81] S. Rahman and O. Hazim. A generalized knowledge-based short-term load-forecasting technique. *IEEE Trans. Power Systems*, 8(2):508–514, May 1993.
- [82] S. Rahman and G. Shreshta. A priority vector based technique for load forecasting. *IEEE Trans. Power Systems*, 6(4):1459–1465, November 1991.
- [83] N.S. Rau. Assignment of capability obligation to entities in competitive markets: The concept of reliability equity. *IEEE Trans. Power Systems*, pages 884–889, 1999.
- [84] D.P. Rutenberg. Risk aversion in stochastic programming with recourse. *Operations Research*, 21:377–380, 1973.
- [85] E.S. Schwartz. The stochastic behavior of commodity prices: Implications for valuation and hedging. *J. of Finance*, 52(3):923–973, 1997.

- [86] G.B. Sheble. Decision analysis tools for genco dispatchers. *IEEE Trans. Power Systems*, 14(2):745–750, May 1999.
- [87] G.B. Sheble and G.N. Fahd. Unit commitment literature synopsis. *IEEE Trans. Power Systems*, 9(1):128–135, February 1994.
- [88] S.N. Siddiqi. Project valuation and power portfolio management in a competitive market. *IEEE Trans. Power Systems*, 15(1):116–121, February 2000.
- [89] C. Singh and J.O. Kim. A frequency and duration approach for generation reliability evaluation using the method of stages. *IEEE Trans. Power Systems*, 8(1):207–215, February 1993.
- [90] C. Singh and J.O. Kim. A continuous distribution approach for production costing. *IEEE Trans. Power Systems*, 9(3):1471–1477, August 1994.
- [91] K. Sinha. Storage strategies. *Energy Risk*, February 2004.
- [92] J.E. Smith and R.F. Nau. Valuing risky projects: Option pricing theory and decision analysis. *Management Science*, 41:795–816, 2003.
- [93] C. Stetson and P. Murray. Power outage risk. *EPRM Publications*, 45, October 2000.
- [94] H.G. Stoll. *Least-Cost Electric Utility Planning*. Wiley, 1989.

- [95] S. Takriti, S. Supatgiat, and L.S-Y. Wu. Coordinating fuel inventory and electric power generation under uncertainty. *IEEE Trans. Power Systems*, 17(1):13–18, February 2002.
- [96] E. Tanlapco, J. Lawarree, and C-C. Liu. Hedging with futures contracts in a deregulated electricity industry. *IEEE Trans. Power Systems*, 17(3):577–582, August 2002.
- [97] J.W. Taylor and R. Buizza. Neural network load forecasting with weather ensemble predictions. *IEEE Trans. Power Systems*, 17(3):626–632, August 2002.
- [98] S. Vemuri, D. Hill, and R. Balasubramanian. Load forecasting using stochastic models. *Proc. 8th Power Ind. Comput. Applicat. Conf.*, pages 31–37, 1973.
- [99] Michael R. Walls. Corporate risk-taking and performance: A 20 year look at the petroleum industry. *Journal of Petroleum Science and Engineering*, 48:127C 140, 2005.
- [100] C. Wolf. The recovery of risk preferences from actual choices. *Econometrica*, 51, Issue 3:843–850, 1983.
- [101] A. Wood and B.F. Woolenbug. *Power Generation Operation and Control*. Wiley, 1996.

- [102] K.J. Worzel, C. Vassiadou-Zeniou, and S.A. Zenios. Integrated simulation and optimization models for tracking indices of fixed-income securities. *Operations Research*, 42(2):223–233, March-April 1994.
- [103] H.Y. Yamin and S.M. Shahidepour. Risk and profit in self-scheduling for gencos. *IEEE Trans. Power Systems*, 19(4):2104–2106, November 2004.
- [104] Z. Younes and M. Ilic. Generation strategies for gaming transmission constraints will the deregulated electric power market be an oligopoly? *Decision Support Systems*, pages 207–222, 1999.
- [105] V.R. Young and T. Zariphopoulou. Pricing dynamic insurance risks using the principle of equivalent utility. *Scandinavian Actuarial Journal*, 2:246–279, 2002.

Vita

Hanjie Chen was born in Shantou City, Guangdong Province, P.R. China. He received a B.S. degree in Electrical Engineering from Tsinghua University, Beijing, China, in July 2000. In August 2000, he entered the Department of Electrical and Computer Engineering at The University of Texas at Austin, Austin, Texas, USA, to pursue his Ph.D. degree. He was granted M.S. degree in May 2002. He worked as a Graduate Intern in Lower Colorado River Authority in Austin, TX from June 2002 to December 2002 and later as a Principal Energy Risk Analyst in the same company from January 2003.

Permanent address: Bixiazhuang Zhongqu Building 29, Room 803
Shantou City, Guangdong Province, P.R. China
515041

This dissertation was typeset with \LaTeX^\dagger by the author.

[†] \LaTeX is a document preparation system developed by Leslie Lamport as a special version of Donald Knuth's \TeX Program.